Functional characterization of the protease ClpQ in transgenic *Plasmodium berghei* in immunologically different murine hosts

INAUGURAL-DISSERTATION
zur Erlangung des Grades eines
Dr. med. vet.
beim Fachbereich Veterinärmedizin
der Justus-Liebig-Universität Gießen

TANJA PAQUET-DURAND

Aus dem Institut für Parasitologie der JLU Gießen

Betreuer: Prof. Dr. rer. nat. Christoph G. Grevelding

und

aus dem Institut für Tropenmedizin der Eberhard-Karls-Universität Tübingen

Betreuer: Prof. Dr. rer. nat. Jürgen F. J. Kun

Functional characterization of the protease ClpQ in transgenic *Plasmodium berghei* in immunologically different murine hosts

INAUGURAL-DISSERTATION

zur Erlangung des Grades eines

Dr. med. vet.

beim Fachbereich Veterinärmedizin

der Justus-Liebig-Universität Gießen

Eingereicht von

Tanja Paquet-Durand

Tierärztin aus Bremen

Gießen 2010

Mit Genehmigung des Fachbereiches Veterinärmedizin der

Justus-Liebig-Universität Gießen

Dekan:	**Prof. Dr. Martin Kramer**
Gutachter:	**Prof. Dr. rer. nat. Christoph G. Grevelding**
	Prof. Dr. rer. nat. Jürgen F. J. Kun

Tag der Disputation: **21.12.2010**

Meinen Eltern gewidmet!

1 TABLE OF CONTENTS

2 LIST OF ABBREVIATIONS

AMA-1	apical membrane antigen 1
ca.	circa
ClpQ	threonine peptidase encoded by *hslV*
cssurrna	C-type small subunit rRNA
DC	dendritic cell
dpi	days post infection
dssurrna	D-type small subunit rRNA
ECM	experimental cerebral malaria
e.g.	example given
fig.	figure
GPI	glycosylphosphatidylinositol
hdhfr	*human dihydrofolate reductase*
hslV	*heat shock locus V*
hslV-KO	*hslV* knockout
i.e.	in explanation
i.p.	intraperitoneally
iRBCs	infected red blood cells
IU	international units
i.v.	intravenously
LB medium/agar	lysogeny broth medium/agar
MyD88	myeloid differentiation primary response gene 88
MyD88-KO	MyD88 knockout
N/A	not applicable
PAMP	pathogen associated molecular pattern
pbeef1aa	5´UTR of *P. berghei* elongation factor 1 alpha (not stage-specific promoter sequence)
PfEMP1	*Plasmodium falciparum* erythrocyte membrane protein 1
PRR	pattern recognition receptor
RBC	red blood cell
RT	room temperature
s.c.	subcutaneously
SOB medium	super optimal broth
SOC medium	SOB with added glucose

spp.	species
tgdhfr	*toxoplasma gondii dihydrofolate reductase*
TLR	Toll-like receptor
vs.	versus
WT	wild type

3 INTRODUCTION AND LITERATURE SURVEY

3.1 General introduction to malaria

3.1.1 Malaria host range and parasite species

Malaria, caused by apicomplexan parasites of the genus *Plasmodium*, is a vector-borne infectious disease, which is transmitted by mosquitoes of the genus *Anopheles*. Many *Plasmodium spp.* are important pathogens for humans as well as for animals. In humans, malaria is caused by five different *Plasmodium spp*., namely *P. falciparum*, *P. vivax, P. ovale, P. malariae,* and by the simian malaria parasite *P. knowlesi*. Besides humans, various birds, rodents, reptiles, and primates can be infected by a total of 199 *Plasmodium spp.* (Martinsen et al. 2008). Usually *Plasmodium spp.* have a narrow host range, i.e. each species has a single genus or even species of host that it can infect (Boothroyd 2009). Although this hampers deductions on human disease from animal model derived data, such models can still be valuable tools for the investigation of processes, which are conserved between parasite species. The potential of the simian parasite *P. knowlesi* to infect humans makes malaria a zoonosis [for a review see Baird (2009)].

3.1.2 The public health impact of malaria

In 2008, a total of about 243 million clinical malaria cases were reported and nearly 863,000 patients died, mostly children under 5 years (World Malaria Report 2009). The disease is widespread within tropical and subtropical regions, especially in sub-saharan Africa, South and Central America, and Southeastern Asia. Malaria poses therefore one of the most important public health problems worldwide. Nevertheless, recent campaigns aim to control, eradicate and eliminate malaria, an option that seems possible in view of intensified funding, new interventional tools, improved global cooperation and a worldwide declining disease prevalence (Global Malaria Action Plan 2008). However, previous experiences have shown that resistance against antimalarial drugs as well as against insecticides to control its mosquito vector may evolve rapidly and unexpectedly, making long-term forecasts regarding development of disease prevalence difficult and ongoing efforts to develop new tools against the malaria parasite necessary (Kilama and Ntoumi 2009). Up to date, there

is no malaria vaccine available, although clinical trials for some vaccine candidates are ongoing. Plasmodia have been proven to be capable of resistance development against all classes of antimalarials used so far. Even though the risk of resistance development can be lowered by using combinations of different drugs, as e.g. in Artemisinin-based combination therapy (ACT), there remains a persistent threat of resistance, which means that new molecules with novel mechanisms of action are continually required (Wells et al. 2009). Further complications may arise through climatic changes, which could even put previously disease-free, temperate areas at risk for malaria spreading. Taken together, malaria remains a serious global health problem, which requires continuous efforts for its control.

3.1.3 Life cycle of the malaria parasite plasmodium

(see even Fig. 1)

Humans (and other vertebrates) are infected with plasmodia by a bite of mosquitoes of the genus *Anopheles*. Following infection, injected sporozoites first migrate to the liver, where they undergo nuclear division, thereby developing into liver schizonts. Eventually, these schizonts release the contained merozoites into the bloodstream. Within the blood stream, parasites immediately invade erythrocytes and develop within these host cells into trophozoites and later into multinucleated, merozoite-containing schizonts. Merozoites of blood schizonts are freed through schizont egress and invade subsequently new red blood cells. The development of the blood stages is responsible for the clinical signs of malaria, a fact that makes them especially important for researchers and healthcare practitioners alike.

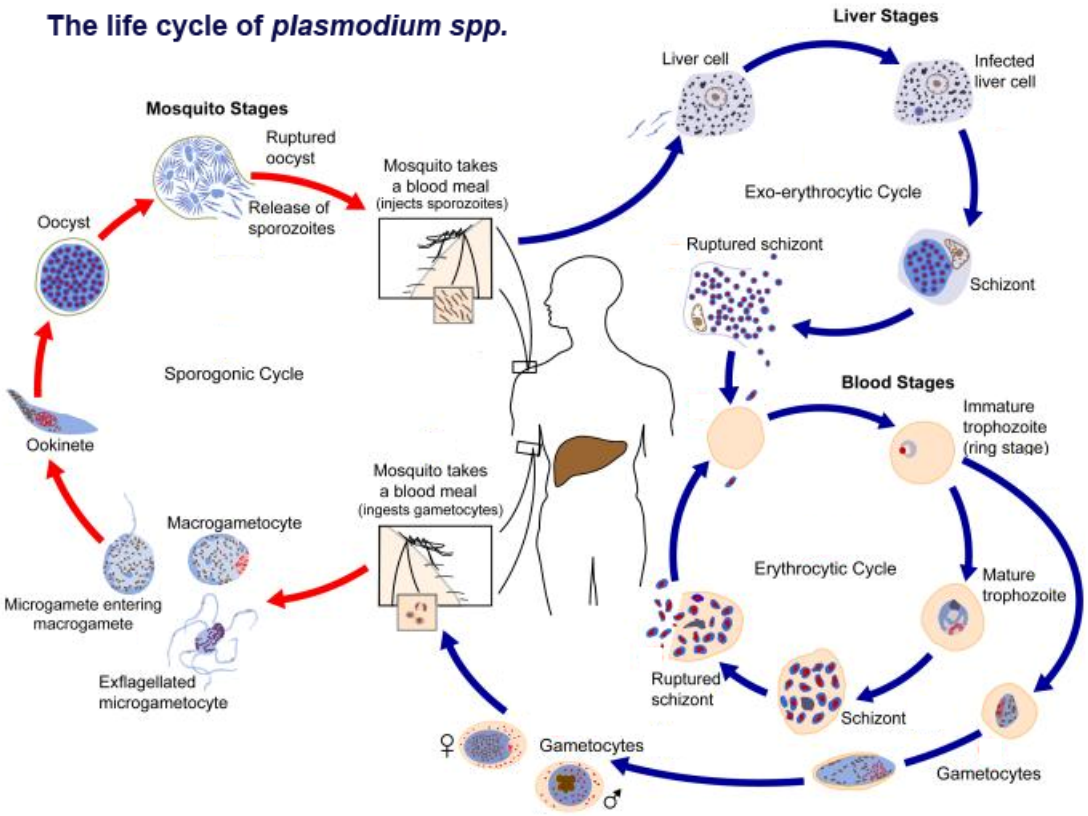

Fig. 1

3.2 Reverse genetics in malaria research

3.2.1 Transfection techniques for plasmodia

The application of reverse genetics strategies to malaria research has facilitated the understanding of many plasmodial gene functions. Genetic modification allows to elucidate gene functions by phenotyping of genetically modified, e.g. knockout parasites. Unfortunately, this approach is hampered by the paucity of information regarding gene regulation in *Plasmodium spp.*. Although precise regulation of protein expression seems to be mandatory in the light of different parasitic stages, a changing environment within the host organisms or virulence-associated processes such as cytoadherence or erythrocyte invasion, the transcriptional regulations of such processes remain poorly understood. Only very few transcription factors have been identified so far, and there is evidence that post-transcriptional regulation may play a significant role in plasmodia (Coleman and Duraisingh 2008, Deitsch et al. 2007). Nevertheless, transfection experiments have still elucidated a variety of gene

functions in *Plasmodium spp.*. Transfection possibilities for malaria parasites are reviewed by de Koning-Ward et al. (2000b) and by Balu and Adams (2007) and are briefly summarized below.

Today it is possible to stably transfect the human parasite *P. falciparum*, the simian parasites *P. knowlesi* and *P. cynomolgi* as well as the rodent parasites *P. berghei*, *P. yoelii*, and *P. chabaudi*. Although it seems favourable to undertake investigations in *P. falciparum*, the transfection of this parasite species is hampered by extremely low transfection efficiencies and difficulties to isolate transfectants with integrated constructs. Although *in vivo* experiments are theoretically possible, analysis of transfected parasites is restricted to *in vitro* investigation. These drawbacks apply to a lesser extend even for the simian parasites. For those reasons many reverse genetic studies in malaria have been done using rodent malaria parasites. Especially the murine malaria parasite *P. berghei*, which is described in more detail in the following section, has proven to be very suitable for genetic manipulations.

3.2.2 The *Plasmodium berghei* model organism in reverse genetics

P. berghei is the most frequently employed malaria model organism in reverse genetics. According to a protocol developed by Janse et al. (2006), transfection efficiencies reach one in 10^{-2} to 10^{-3}, compared to one in 10^{-6} in *P. falciparum*. The model allows transfection of linear instead of circular DNA, which facilitates genomic integration via single or double-crossover. A multitude of established vectors with different reporter genes and promoter types is available. Better parasite growth rates allow the isolation of transfected parasite clones with stably integrated constructs within a few weeks, compared to several months in *P. falciparum*, which facilitates medium throughput experiments. Furthermore, the effects of genetic manipulations can be assessed *in vivo*. Disadvantages are the unclear relevance from investigations in the murine host for human disease, a paucity of selectable markers, the limited number of parasites that can be recovered per experiment restricting their biochemical characterization, and the impracticality of long-term *in vitro* culture. Nevertheless, the *P. berghei* model still may reveal valuable insights into host-pathogen interactions especially regarding conserved biochemical pathways.

P. berghei transfection is achieved by electroporation of schizonts, using the Amaxa™ Nucleofector device (Janse et al. 2006). Transfected parasites are injected

i.v. into a mouse and subsequently selected from the total parasite population by antibiotic treatment of this mouse. This selection is facilitated by a selectable marker sequence that is part of the transfected DNA and confers resistance to the selective agent, usually pyrimethamine or WR99210 (see even fig. 3 in section 5.3.6). Subsequent phenotyping of cloned, transfected parasites facilitates conclusions regarding the function of modified genes. In this thesis, characterization of the parasite-specific protease *hslV* was facilitated by phenotyping of *hslV* knockout (*hslV*-KO) and knockout rescue parasites.

3.3 The protease ClpQ encoded by the gene *hslV*

3.3.1 The function of ClpQ in protein degradation

All living cells rely on intracellular proteolysis to remove, tagged, unneeded or damaged proteins, and to maintain protein homeostasis. For *Plasmodium spp.* regulation of protein turnover is especially important due to high replication rates of the blood-stage parasites, stress on proteins caused by increased temperature (fever of the host), the large size of plasmodial proteins, the high frequency of low complexity regions within the plasmodial genome (Kreidenweiss et al. 2008), and a high degree of posttranscriptional control of protein levels (Deitsch et al. 2007).

During evolution, different organisms have developed distinct proteolytic machineries to control protein turnover. In eukaryotes, archaea, and some bacteria proteolysis is accomplished by the 20S proteasome, a large ATP-dependent, multisubunit proteolytic complex, whereas the majority of bacteria possess several different proteolytic enzymes, amongst others a proteasome-like heat shock protein encoded by *heat shock locus V*, *hslV* (Groll et al. 2005). Despite this general taxonomic classification, it has been shown that the two degradation mechanisms appear not mutually exclusive, but are both present in some *protozoa*, e.g. in *Plasmodium spp.* (Gille et al. 2003). Mordmüller et al. (2006) discovered that the plasmodial proteasome is catalytically active and expressed throughout the life cycle, whereas *hslV* is expressed exclusively during late parasitic stages. The *hslV*-coding sequence is highly conserved between different *Plasmodium spp.*, which indicates purifying selection on this gene suggesting an essential function of *hslV*.

3.3.2 Molecular structure of ClpQ

The gene *hslV* codes for the threonine peptidase ClpQ, which shares 20% similarity and a conserved fold with the β subunits of the proteasome (Bochtler et al. 2000). The *hslV* gene product consists of a 37aa (18kDa) long pro sequence, which targets the molecule into mitochondria (Tschan et al. 2010), followed by the 170aa (23kDa) mature protease, which is activated by removal of the targeting signal. The mature protease forms a dodecameric barrel-like structure. Analogous to the 20S proteasome its openings possess polar caps, here represented by the ATPase HslU, a member of the Hsp100 (Clp) family of ATPases, which actively channels proteins destined for degradation into the interior of the *hslV* complex (Bochtler et al. 2000).

Due to its highly conserved sequence among *Apicomplexan spp., hslV* appears to play a fundamental role in plasmodial cell metabolism. Its absence in the mammalian host makes it an attractive target for future interventional approaches especially since potent and selective inhibitors can be designed against this molecule (Elofsson et al. 1999, Powers et al. 2002).

This thesis investigates its function in a murine malaria model, by generating *hslV*-deficient *P. berghei* parasites and subsequent characterization of these parasites.

3.4 Host parasite interactions during plasmodium infections

3.4.1 Introduction

Symptoms caused by malaria include intermittent fever, shivering, arthralgia, anemia, metabolic acidosis, organ dysfunction and, in cases of cerebral malaria, convulsions and coma (Stich 2009). The severity of the clinical picture can vary considerably and is determined by an interplay of many host- and parasite-associated factors, such as the immune status of the host, parasitemia, and virulence of the infecting parasite strain.

Symptoms are mainly caused by a parasite-induced proinflammatory immune response (Franklin et al. 2009). On the other hand, malaria leads even to a partial immunosuppression of the host (Urban and Todryk 2006). The reasons for this regulation of both innate and acquired immune responses remain unclear. Despite the fact that parasites can persist within the host for extended periods of time, immunity against plasmodia develops only slowly, and long-term immunity requires

repeated pathogen exposure (Langhorne et al. 2008). Plasmodia are highly adapted to the environment within their host. Their complex life cycle, which comprises multiple, immunologically distinct forms, enables them to evade or even suppress host immune responses, despite the induction of both the innate and the adaptive immune system (Coban et al. 2007). These complex interactions between parasite and immune system of the host make the development of new therapeutic or prophylactic tools like antimalarial drugs or vaccines especially challenging. Therefore, a better understanding of host-parasite-interactions seems mandatory to find new targets for pharmacological or prophylactic intervention.

3.4.2 The eukaryotic immune system

The function of the eukaryotic immune system is to protect the organism from disease by recognizing and eliminating pathogens or tumour cells. It is divided into the innate (unspecific) and the adaptive (specific) immune system. In view of vaccine development efforts, malaria research was until recently mainly focused on adaptive immunity, but there is increasing evidence that innate immune mechanisms are of critical importance for malaria protection and that a comprehensive understanding of those mechanisms is of importance for the development of new anti-malarial agents (Stevenson and Riley 2004).

The innate immune system comprises cells and mechanisms that protect the organism in a non-specific manner. It provides an immediate first line defence against invading pathogens and is the main activator of acquired immune responses. Important components of the innate immune system are phagocytic cells (macrophages, monocytes and neutrophils), cells that release inflammatory mediators (basophils, mast cells and eosinophils) and natural killer cells as well as soluble mediators such as acute phase proteins, cytokines and complement components (Delves and Roitt 2000).

3.4.3 PAMPs and pattern recognition receptors

The innate immune system senses invading pathogens through so-called pattern recognition receptors (PRRs). PRRs are activated through pathogen-associated molecular patterns (PAMPs), i.e. small molecular motifs conserved within distinct classes of pathogens, which are not expressed in the host organism itself (Medzhitov 2007). PRRs are divided into different groups, most importantly the Toll-like receptors

(TLRs), NOD-like receptors (NLRs), RIG-I-like receptors (RLRs) and C-Type lectin receptors (Ishii et al. 2008, Rasmussen et al. 2009). All TLRs except TLR3 depend on a common adapter molecule named myeloid differentiation primary response gene 88 (MyD88) to activate downstream signaling cascades. Upon TLR ligand binding, MyD88 mediates the activation of nuclear factor-kappaB (NF-κB), interferon regulatory factors (IRFs) and mitogen-activated protein kinases (MAPKs), all members of pathways that stimulate inflammatory responses, such as induction of pro-inflammatory cytokines and interferon-inducible genes (Rasmussen et al. 2009, Waters et al. 1997). Due to this central role of MyD88 for TLR-signaling, TLR involvement in pathogenic processes can be assessed by comparison of this process in a normal compared to a MyD88-deficient host, i.e. intact and MyD88 knockout (MyD88-KO) mice.

3.4.4 The role of PRRs and PAMPs during *Plasmodium* infections

It still remains unclear which plasmodia-specific PAMPs lead to TLR activation during plasmodium infections. Currently the two main candidates for plasmodial PAMPs are the plasmodial pigment hemozoin and the glycosylphosphatidylinositol (GPI) anchor. GPIs are eukaryotic glycan molecules that anchor surface proteins into plasma membranes. Plasmodial GPIs are structurally distinct from vertebrate GPIs and considered as plasmodial PAMPs, which evoke a proinflammatory immune response by signaling via TLR2 and 9 (Coban et al. 2007a, Gowda 2007, Arrighi and Faye 2009).

While GPI is believed to evoke a proinflammatory response, the role of hemozoin in host-parasite interactions remains unclear. Urban and Todryk (2006) claim that hemozoin modulates dendritic cell (DC) function of the host, leading to an impaired induction of adaptive immune responses, whereas Griffith et al. (2009) found a proinflammatory immune response in stimulation studies with synthetic hemozoin. Coban et al. (2005) report that hemozoin is modulating the innate immune response by binding to TLR9. A hemozoin-mediated TLR9 activation was also proposed by Parroche et al. (2007) who propose that the activation is not triggered by hemozoin itself, but by hemozoin-presented plasmodial DNA, a thesis that is contradictory to the results of Griffith et al. (2009). Despite inconsistencies of results, these and other studies nevertheless suggested hemozoin as a candidate for a plasmodial PAMP.

To date Toll-like receptors (TLRs) seem to be the most important PRR group during the innate immune response. Another PRR that is suspected to be involved in parasite-induced immunosuppression is the class B scavenger receptor CD36. Whether CD36 contributes to innate host defence or rather to pathophysiology remains controversial (Areschoug and Gordon 2009). CD36 is a receptor for *Plasmodium*-infected red blood cells (iRBCs). In *P. falciparum* the main ligand for CD36 is *Plasmodium falciparum* erythrocyte membrane protein 1 (PfEMP1). PfEMP1 is thought to mediate sequestration of iRBCs, which in turn may lead to increased disease severity and enhanced parasite survival [reviewed by Serghides et al. (2003). In *P. berghei,* PfEMP1 is not present, but Franke-Fayard et al. (2005) showed that CD36-mediated sequestration of iRBCs even occurs in the absence of PfEMP1. Furthermore, CD36 acts as a co-receptor for the TLR2/TLR6 complex (Akashi-Takamura and Miyake 2008), which means that signaling pathways involving CD36 could also be impaired in MyD88-KO mice.

Taken together these facts about the innate immune response suggest that TLRs play a major role in innate immune responses to malaria parasites. For this reason, their involvement in mediation of the phenotypic differences between WT- (wild type) and *hslV*-KO parasites was investigated in this thesis by infection of MyD88-KO mice.

4 HYPOTHESIS AND DISSERTATION OBJECTIVE

This thesis aims to characterize the function of the threonine peptidase *hslV* in *Plasmodium spp.* by means of reverse genetics. Since the highly conserved sequence of *hslV* suggests an essential role of the protease, investigations aimed to clarify, whether *hslV* is essential for the malaria parasite, and to investigate its possible function in the rodent model *P. berghei*. To achieve this goal *hslV*-KO-parasites were generated and characterized with respect to physiological and immunological parameters.

To prove that the *hslV*-knockout itself led to the observed phenotypic changes in the knockout-parasites, rescue-parasites, i.e. *hslV*-KO-parasites, cotransfected with a *hslV*-expression-cassette in a different genomic locus were generated. To control for effects caused by alteration of the cotransfected locus (*c*- or *d-ssurrna*), a mock-transfected parasite line, containing a transfection construct, identical to the rescue construct, but lacking the *hslV*-coding-sequence was generated and phenotypes of both mock and rescue parasites compared to the *hslV*-KO-parasites.

5 MATERIALS AND METHODS

A detailed list of reagents can be found at the end of the chapter.

5.1 General methods for molecular cloning

5.1.1 Plasmid transformation

For amplification 50ng plasmid DNA were mixed with 50µl competent bacteria (i.e. XL-10 Gold (Stratagene) or TOP-10 (Invitrogen) chemically competent *Escherichia coli* cells), incubated on ice for 10min and subsequently heat-shocked at 42°C for 45s. Immediately thereafter, 250µl SOC medium was added; the culture was shaken at 37°C for 60min and then streaked out on a LB agar plate containing the appropriate antibiotic for selection of the transformed plasmid (ampicillin or kanamycin).

5.1.2 Plasmid-DNA isolation

Depending on the required amount of DNA, plasmid DNA was isolated using either the "peqGOLD HP Plasmid Miniprep Kit I" (Peqlab) or the "Qiagen® Plasmid Maxi Kit" (Qiagen) according to the manufacturer's instructions.

Basic principles of the used kits:

In both procedures plasmid DNA is selectively lysed using a modified alkaline lysis procedure and extracted by adsorption onto a silica-gel spin column followed by washing steps. For small scale preparations (Mini-Preps) DNA was subsequently eluated under low salt conditions. For large scale preparations (Maxi-Preps) DNA was eluted using high-salt buffer conditons and finally concentrated and desalted by isopropanol precipitation.

5.1.3 Measurement of DNA content of samples

To determine the DNA content of plasmid or genomic DNA prior to ligation, transfection, PCR, or sequencing, DNA concentration was quantified by measuring the samples´ absorbance at 260 nm using a NanoDrop® ND-1000 spectrophotometer

(NanoDrop Technologies, Inc., Wilmington USA) according to the manufacturer's instructions.

5.1.4 DNA ligation

Prior to ligation, restricted DNA fragments were separated by agarose gel electrophoresis, cut out of the gel and purified using the "NucleoSpin® Extract II Kit" (Macherey-Nagel) according to the manufacturer's instructions.

For ligations at two identical restriction sites vector DNA was dephosphorylated using "rAPid Alkaline Phosphatase®" (Roche).

Maximal possible amounts of insert and vector DNA were used in the ligation reaction as calculated using the following formula, which determines the amounts of DNA for a 10:1 insert: vector ratio:

INSERT MASS [ng] = INSERT LENGTH [bp] / VECTOR LENGTH [bp] x VECTOR MASS [ng] X 10

DNA was ligated overnight at 16°C using T4 DNA ligase (Fermentas). Subsequently, ligation reactions were directly transformed into competent bacteria for amplification. Transformants containing the desired insert were identified by colony PCR, restriction enzyme analysis, and sequencing. For colony PCR a standard PCR master mix, as described in section 5.4.3, was used. Primers and thermocycler settings for the different products are given in table 1 (section 5.2.4) and in section 5.4.4 respectively. The PCR reactions were inoculated with one bacterial colony serving as template. After inoculation, residual colony material was transferred to a defined area of a selective agar plate to spare the respective clones for future purposes. Plasmid DNA from positive clones was analyzed by restriction enzyme analysis and/or sequencing of the insert.

5.1.5 Sequencing

To confirm their correct sequences, all cloned fragments were sequenced on an ABI PRISM® 3100 Genetic Analyzer (Applied Biosystems).

Sequencing samples were generated using the "BigDye® Terminator v1.1 Cycle Sequencing Kit" and the following reaction mix:

2µl 2.5x Ready Reaction Premix, 4µl 5x BigDye Sequencing Buffer, 3.2 pmol primer, 200ng template, water up to 20µl

Thermocycler: Biometra UNO II

Settings: (94°C – 10s, 50°C – 5s, 60°C – 4min, 24 cycles), 72°C 7 min

PCR products were subsequently purified to remove unincorporated dye terminators using Centri-Sep™ spin columns (Applied Biosystems) according to the manufacturer's instructions.

Sequences were analyzed using the BioEdit sequence alignment editor.

5.2 Cloning of transfection vectors

5.2.1 General vector description

Generally, selection of transfected parasites is facilitated by the introduction of a selectable marker that confers resistance to pyrimethamine, such as the *dihydrofolate reductase* (*dhfr*) gene from *Toxoplasma gondii* (*tgdhfr*) or the human *dhfr* gene (*hdhfr*). *hdhfr* confers not only pyrimethamine resistance, but also resistance to the antimalarial drug WR99210, which facilitates its use as a second selectable marker in *tgdhfr*-transfected parasites (Janse et al. 2006).

The initial *hslV*-KO construct contained the selectable marker *hdhfr* flanked by ca. 500bp of *pbhslV* 5´ and 3´UTR sequences to facilitate integration at the genomic *hslV* locus via double crossover.

To rescue this knockout, it became necessary to clone a second knockout vector, similar to the first one, but containing *tgdhfr* instead of *hdhfr*.

Parasites transfected with this second, *tgdhfr*-selectable knockout vector allowed the introduction of *hdhfr* as a second selectable marker to select for cotransfected parasites, additionally containing the rescue/mock construct with WR99210.

The rescue vector contained two expression cassettes, one for the selectable marker *hdhfr* and another for *pfhslV* as well as a ca. 2KB long homologous sequence to facilitate integration into the genome of *P. berghei* at the *cssurrna* or *dssurrna* gene locus via single crossover. The mock vector was identical to the rescue vector, but lacked the *pfhslV* sequence.

5.2.2 Maps of transfection vectors

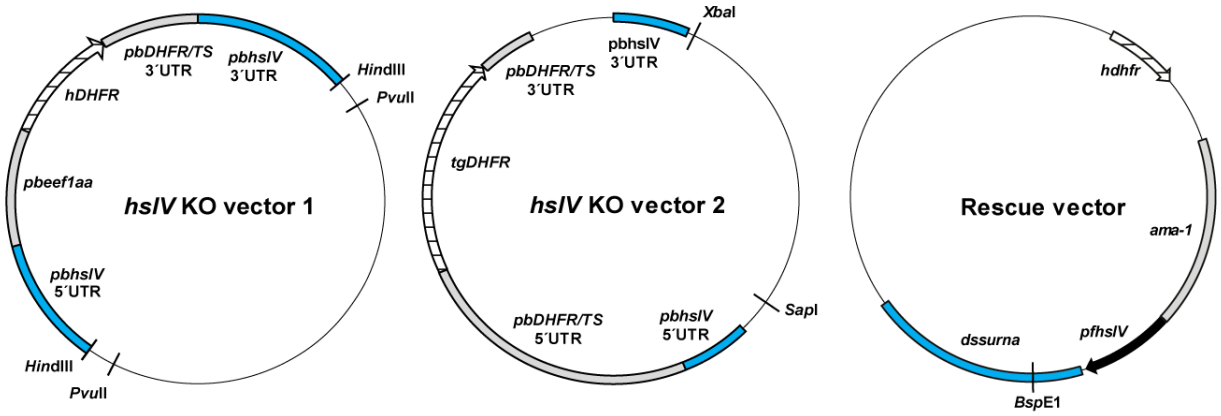

Fig. 2: Transfection vectors.

Left: first knockout vector, middle: second knockout vector used for rescue cotransfection, right: rescue construct [mock vector = identical to rescue vector, but without *pfhslV* sequence (black segment)]. Indicated restriction sites were used to linearize the constructs prior to transfection.

5.2.3 Plasmids for cloning of transfection vectors

The standard *P. berghei* transfection vectors pl0005, pl0006, pl0010 and pl0031 were obtained from the MR4, ATCC®, Manassas, Virginia, USA. All those vectors are MR4 deposits of A. Waters, Leiden Malaria Research Group, LUMC, Netherlands (website reference: *P. berghei* - Plasmids for genetic modification).

5.2.4 Cloning procedure

Homologous *pbhslV* sequences were amplified from genomic *P. berghei* DNA and *pfhslV* from plasmid DNA using the primers listed in table 1. PCR fragments were subsequently cloned into the pCR®2.1-TOPO® Vector (Invitrogen) and sequenced to verify correct amplification (sequencing was performed as described in section 5.1.5). Except for the *pbhslV* 3´UTR, fragments were cloned using primer-specific restriction sites.

For the first, *hdhfr*-selectable knockout vector, the amplified *pbhslV* 3´UTR fragment was modified by cloning it into the pCR®2.1-TOPO® vector (Invitrogen) and subsequent excision with *Eco*RI. *pbhslV* 5´UTR and 3´UTR sequences were subcloned into pl0005. The resulting plasmid contained a cassette for the expression

of the selectable marker *hdhfr* under the control of the constitutively active *pbeef1aa* promoter flanked by *pbhslV* 5´UTR and 3´UTR sequences.

For the second knockout vector with *tgdhfr* as selectable marker, the 5´UTR of *pbhslV* was amplified from plasmid DNA using the same primer sequences as for the first vector, but with *Kpn*I instead of *Hin*dIII/*Pst*I restriction sites. The resulting fragment was cloned into pl0031. The *pbhslV* 3´UTR sequence from the construction of the first knockout vector was cut out of pCR®2.1-TOPO® using the enzymes *Nde*I and *Xba*I. The resulting plasmid contained a cassette for the expression of the selectable marker *tgdhfr* under the control of the 5´*pbdhfr/TS* promoter sequence, which is active in old trophozoites, schizonts, and sexual parasite stages. This expression cassette is flanked by *pbhslV* 5´UTR and 3´UTR sequences. Parasites transfected with either of those two vectors can be selected by pyrimethamine treatment of the infected mice.

To clone the rescue vector, first total RNA of *P. falciparum* parasite extracts was reverse transcribed with SuperScript® III Reverse Transcriptase (Invitrogen). *pfhslV* was amplified using the primers listed in table 1, cloned into the pCR®2.1-TOPO® Vector (Invitrogen) and subcloned into pl0010, using the primer-specific restriction sites. The resulting expression cassette contains the schizont-specific promoter *ama-1* and the *pfhslV*-cDNA sequence of *pfhslV*. The stage-specific promoter was chosen, since plasmodial *hslV* is expressed during late stages, only. The *tgdhfr*-selectable marker of this plasmid as well as its 5´UTR and 3´UTR sequences were removed by *Eco*RV-*Hin*dIII restriction and replaced with the *hdhfr* sequence from pl0006, including its constitutively active promoter *pbeef1aa* and its 3´UTR 3´*pbdhfr/TS*. The *hdhfr*-selectable marker facilitates the selection of transfected parasites from a pyrimethamine-resistant parasite population using the antimalarial compound WR99210. The rescue construct integrates into the *c*- or *dssurrna* locus via single crossover and can be lost again, if parasites are not kept under constant drug pressure. To confirm that phenotypic findings obtained from rescue vector-transfected parasites are not provoked by this drug treatment, a mock vector identical to the rescue vector, but lacking the *pfhslV* sequence, was cloned using the same approach as described above.

Name	Sequence	Restriction site (uncapitalized)
pbhslV 5´UTR-1st KO for	5´ - TTTa agcttCGTCTTTTGGAATG - 3´	*Hin*dIII
pbhslV 5´UTR-1st KO rev	5´ - TTTctgca gCGCTTAAGTGTAGAAAAC - 3´	*Pst*I
pbhslV 5´UTR-2nd KO for	5´ - TTTggtaccCGTCTTTTGGAATG – 3´	*Kpn*I
pbhslV 5´UTR-2nd KO rev	5´ - TTTggtaccCGCTTAAGTGTAGAAAAC - 3´	*Kpn*I
pbhslV 3´UTR (1st+2nd KO) for	5´ - AAAtctaga CGAATCATAACTTTATATGTG - 3´	*Xba*I
pbhslV 3´UTR (1st+2nd KO) rev	5´- TTTaagcttTTCAGGCGTTTATGCATTTG-3´	*Hin*dIII
pfhslV-cDNA for	5' - TTTggatccAACAACTAATTATTCGAAGG - 3'	*Bam*HI
pfhslV-cDNA rev	5' - TTTggtaccCTGACATCCTCTTGATTAG - 3'	*Kpn*I

Table 1: Primers for cloned sequences (small letters indicate restriction sites attached to the primers)

5.2.5 DNA preparation for transfection

Double-crossover constructs were linearized by two restriction enzymes at the ends of the target sequence as listed below (removal of plasmid backbone). Single crossover constructs were linearized at one site within the target sequence as listed below.

Construct	Integration event	Restriction site(s)
hdhfr-KO	Double crossover	*Hin*dIII+*Pvu*II
tgdhfr-KO	Double crossover	*Xba*I+*Sap*I
Rescue	Single Crossover	BspE1
Mock	Single Crossover	BspE1

Per transfection 8µg of DNA was digested overnight in portions of 3µg per reaction with 30U/reaction of each of the enzymes using appropriate buffer and temperature conditions to ensure complete digestion.

Subsequently reactions were pooled, and the DNA was precipitated with 0.1 volume of 3M NaAc, pH 5.2, and 2.5 volumes of 96% ethanol for 2 hours at room temperature or overnight at -20°C and centrifuged (17,000g, 15min, 4°C) to obtain the DNA pellet.
DNA pellets were washed with 200µl of 70% ethanol and resuspended in H_2O to a concentration of 1 µg/µl.

5.3 Parasitological methods

5.3.1 Selection of mouse strains and parasites

All animal work was conducted in accordance with European regulations and approved by the local state authorities (Regierungspräsidium Tübingen). For routine parasite propagation, transfections and cloning CD1^{TM} outbred mice were used. The strain was chosen because of the robust constitution and big size of the animals.
To assess the genetic influence on immune responses growth assays were performed using CD1^{TM}, BALB/c, C57BL/6 and MyD88-KO mice (on the genetic background C57BL/6). All animals, except the MyD88-KO mice were purchased from Charles River Laboratories (Kisslegg) and kept in a conventional open facility. The MyD88-KO mice were a kind gift of Dr. Uwe Klemm (Max-Planck-Institut f. Infektionsbiologie, Berlin, Germany). They were kept under sterile conditions in individually ventilated cages.
All experiments were conducted using *P. berghei* parasites of the ANKA strain (Bafort et al. 1968). Parasites were obtained from A. Walliker (Institute of Cell, Animal, and Population Biology, University of Edinburgh, United Kingdom).

5.3.2 Mouse infections

Mice were infected with blood, containing malaria parasites, diluted in parasite medium or PBS or with cryopreserved parasites directly after thawing. Parasites were administered either intravenously or intraperitoneally. When an exact inoculum size was required or only few parasites were present in the inoculum parasites were injected i.v. (e.g. for transfection, cloning, or growth assays), for all other purposes parasites were administered i.p..

5.3.3 Giemsa staining of blood smears

To determine the parasitemia, dried thin blood smears were briefly fixed in 100% methanol, air-dried and stained for 20min in a 20% Giemsa solution (Giemsa stock diluted with Sörensen staining buffer, i.e. 3.7mM KH_2PO_4, 0.62mM $Na_2HPO_4 \cdot 2H_2O$, pH adjusted to 7.2 with NaOH). The staining solution was filtered prior to use, (folded filter MN615, Macherey-Nagel, Art.-No. 531 024).

5.3.4 Parasite retrieval

At the desired parasitemia 0.5ml to 1ml blood per mouse was taken by cardiac puncture under anesthesia. The blood was immediately mixed with approximately 100µl heparin stock solution (i.e. 0.5ml Liquemin N 5000 diluted in 25ml parasite medium without fetal calf serum = 200IU/ml). Following this, mice were immediately sacrificed by cervical dislocation. The infected blood was then used for the desired purpose such as schizont culturing, DNA or protein extraction or cryopreservation of parasites.

5.3.5 Cryopreservation of parasites

Freshly taken parasite-infected blood was mixed 1:1 with a glycerol/PBS solution (30% glycerol; v/v; containing 5% heparin stock solution of 200IU/ml), the mixture was kept on ice for 5-15min and then frozen at -80°C.

5.3.6 Parasite transfection

Parasites were transfected as previously described (Janse et al. 2006)

The method is described in the following sections (for an overview see fig. 3).

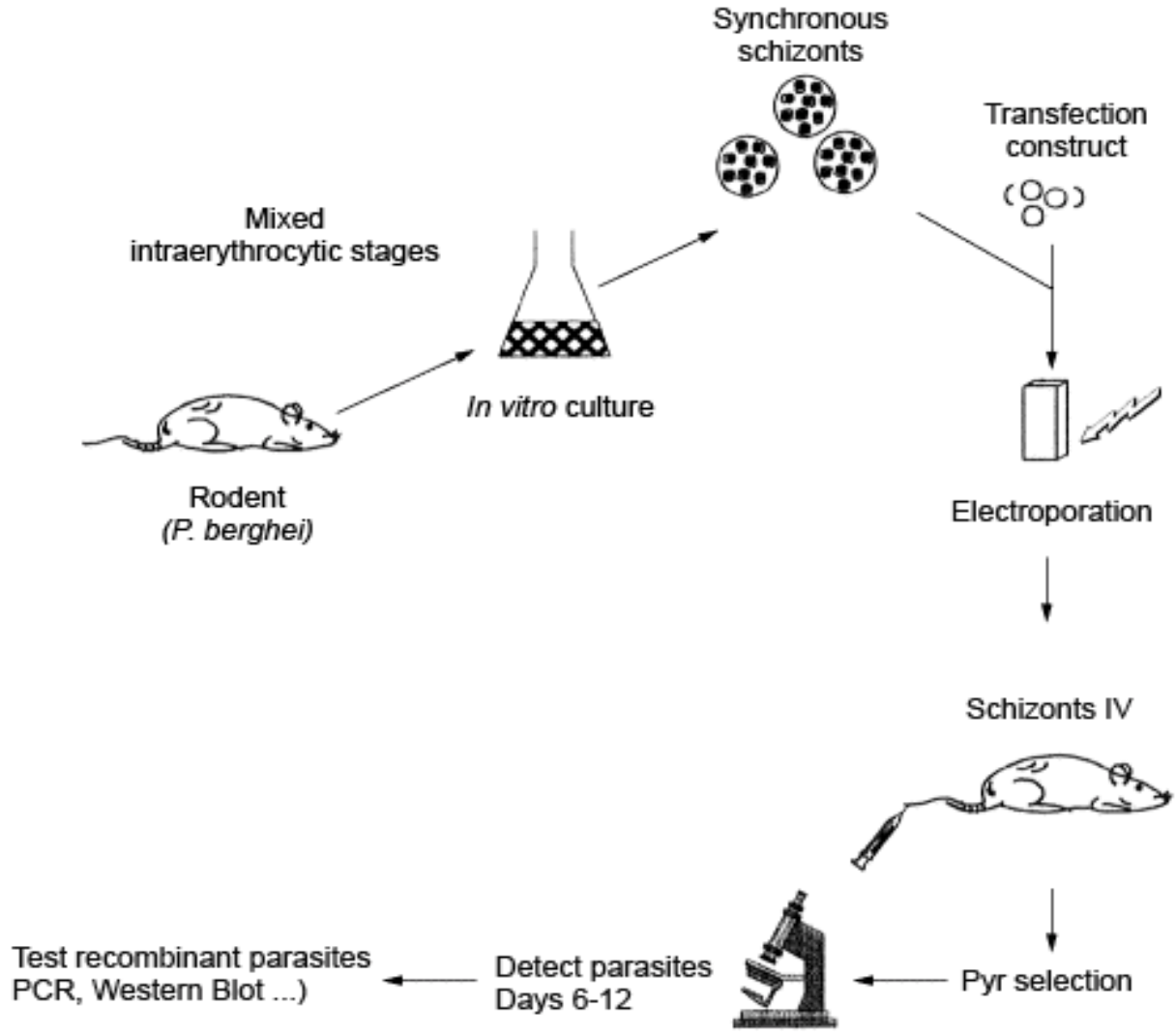

Fig. 3: Overview over the *P. berghei* transfection protocol [modified after (Tomas et al. 1998)].

5.3.6.1 Schizont culture - Rationale for schizont culturing

In *P. berghei* the schizont stage is most suitable for transfections. The schizont fraction of a mixed blood-stage parasite population can be increased by culturing the parasites *in vitro* over night. Since parasites have a circadian rhythm and develop over night into schizonts that do not rupture under *in vitro* conditions, overnight

cultures yield a parasite population mainly consisting of schizonts, which is most suitable for transfection experiments (Janse et al. 2006).

5.3.6.2 Parasite medium

For short-time *in vivo* culturing of *P. berghei* parasites prior to transfection the following medium was used [modified after (Waters et al. 1997)]:

Premix:

500ml RPMI-1640 Medium with $NaHCO_3$

12,5ml HEPES solution, 1M

500µl liquid Gentamicin (50mg/ml)

5ml L-Glutamine solution, 200mM (stored in aliquots at -21ºC)

The premix was stored at 4°C. Immediately prior to use, it was warmed to 37ºC and "Fetal Bovine Serum GOLD" was added to a final concentration of 25% (v/v).

Prior to its first use the fetal bovine serum was inactivated for 30min at 56°C and subsequently stored in 10ml aliquots.

5.3.6.3 Culturing technique

To set up the culture, 0.6-1.0ml infected blood was collected from a donor mouse with a parasitemia of 1-3%. Blood was collected between 10am and 4pm.

Upon collection, the blood was mixed with an equal amount of complete culture medium containing 5% heparin stock-solution (200IU/ml). Cells were then pelleted by centrifugation (8min, 200g), the supernatant was discarded, and the cells resuspended in complete culture medium in a 250ml bottle ("PS-Vorratsflasche", Neolab). For 1 ml blood, 30ml complete culture medium were used. The bottle was incubated for 15min with the lid loosely closed in an incubator with low oxygen tension (37°C, 5% CO_2, 5% O_2, 90% N_2). For overnight culturing, flasks were firmly closed and put at 37°C on a rotor to keep cells in suspension.

5.3.6.4 Histodenz® stock solution for gradient centrifugation medium

138g Histodenz® powder was dissolved in 500ml buffered medium, autoclaved, and stored at 4ºC (Buffered medium: 5mmol/l Tris/HCl / pH 7.5, 3mmol/l KCl, 0.3mmol/l Ca-Na_2EDTA). For the working solution 55% (v/v) Histodenz® stock solution was mixed with 45% sterile-filtered PBS.

5.3.6.5 Centrifugation Procedure

The purification procedure was started between 7am and 9am. The culture suspension containing the schizonts was transferred to 50ml falcon tubes, and 10ml of Histodenz® working solution per tube was added to the culture medium resulting in a sharp contrasting line between the two suspensions. The tubes were then centrifuged for 20-30 min at 200g at room temperature in a swing-out rotor. Using a transfer pipette the brown parasite layer at the interface between the two suspensions was collected into a 10ml tube and approx. 4ml culture medium, obtained from the top of the gradient, was added. Parasites were now pelleted by centrifugation (200g, 8min, normal break setting). After this centrifugation, the supernatant was discarded and the schizont pellet resuspended in 1ml of culture medium per transfection. A schizont culture containing 1ml blood was used for up to four transfections.

5.3.6.6 Nucleofector solutions

Nucleofector solutions were obtained from Amaxa GmbH (Cologne, Germany). For the transfection of the first, *hdhfr*-selectable, knockout construct "Human-T-Cell nucleofector solution" was used. The second knockout construct (using *tgdhfr* as a selectable marker), as well as rescue and mock vector were transfected using "Parasite 2 nucleofector solution" which became available at that time.

5.3.6.7 Transfection procedure

For transfection, cells were pelleted by centrifugation (10s, 17,000g) and the supernatant discarded. Parasite pellets were immediately resuspended in 100µl of nucleofector solution containing 5-10µg DNA, prepared as described in section 5.2.5. The parasite-DNA-buffer solution was transferred to a cuvette and transfected using protocol U33 of the Amaxa® nucleofector device. Directly after electroporation 100µl of culture medium were added, and the solution was immediately injected into the tail vein of a CD1™ outbred mouse.

5.3.6.8 Drug selection of transfected parasites

Drug selection was facilitated by the resistance genes *hdhfr* or *tgdhfr* as parts of the plasmid vector (for a detailed description see section 5.2.1). Transfected parasites

were left without drug pressure for a period of 24h. For selection, transfected parasites were treated with pyrimethamine by administration of the drug to infected mice via the drinking water from day 1 to day 7. The drinking water was prepared from a 100x pyrimethamine stock-solution (pyrimethamine dissolved in DMSO to a final concentration of 7mg/ml) diluted with tap water (pH adjusted to 3.5-5.0, using 5M HCl solution). According to the protocol, the drinking water was freshly prepared for each transfection (or in cases of prolonged treatment once weekly).
For WR99210 selection, mice were injected subcutaneously with the drug on three consecutive days starting 24 hours after transfection (WR99210 injection solution: WR99210 dissolved in DMSO and diluted in a 70% DMSO, 30% H_2O solution to a final concentration of 240µg/100µl). Per treatment 100µl of this solution/animal (with a bodyweight between 10 and 33g) was injected s.c..

5.3.7 Parasite Cloning

Parasites were cloned by limiting dilution (Waters et al. 1997). Mice were inoculated so that the number of clones was Poisson-distributed with a mean $\lambda \leq 0.5$, estimated by counting animals that did not develop parasitemia.
Parasitemia and RBC count in blood with a parasitemia of ca. 1% were determined as described below, and blood was diluted in 160µl parasite medium to obtain ≤50% of animals that develop parasitemia after i.v. injection (generally, 2 microscopically detectable parasites per inoculum). Within 2 hours after calculating parasite numbers, parasite dilutions were injected i.v. into uninfected CD1^{TM} outbred mice.
Parasitemia was determined by counting at least 2,000 cells on a Giemsa-stained slide using a light microscope (staining protocol see section 7.3.3). The number of erythrocytes/µl blood was assessed using a Neubauer chamber. Prior to cell counting leucocytes were lysed by incubating 2µl of blood with 400µl Hayem´s reagent for 5min. Subsequently, the chamber was filled, fluid allowed to settle for 5min, and cells within five big squares were counted. The total number of cells in five squares multiplied by 10,000 equates the number of erythrocytes/µl blood.

5.3.8 *In vivo* growth assays

For assessment of parasite growth rates mice were intravenously injected with 1000 mixed blood-stage parasites. Parasite counting (parasitemia and RBC count) and

preparation was done as described for the cloning procedure. Following infection, the parasitemia of the animals was determined every 24 hours on Giemsa-stained blood smears (staining protocol see section 5.3.3). Survival times of the animals were recorded. Animals with definitive symptoms of cerebral malaria, such as seizures or torticollis or with severe prostration (inability to walk) were killed and recorded as death events.

5.4 Molecular methods for assessment of parasite phenotypes

5.4.1 Isolation of genomic DNA

Genomic parasite DNA was extracted using the "QIAamp DNA Blood Mini Kit" (Qiagen, Hilden, Germany) according to the manufacturer's instructions. The kit procedure comprises an initial lysis step, followed by DNA adsorption onto a silica-gel spin column and two subsequent washing steps. Finally, DNA is eluated under low salt conditions.

If parasites were extracted from more than 200µl blood, saponin lysis was performed prior to extraction to avoid clogging of the column (for a description of the lysis procedure see section 5.4.7). For DNA extraction leucocytes were not removed from the blood. Parasite DNA was subsequently genotyped using the primers listed in table 2 (see even fig. 4).

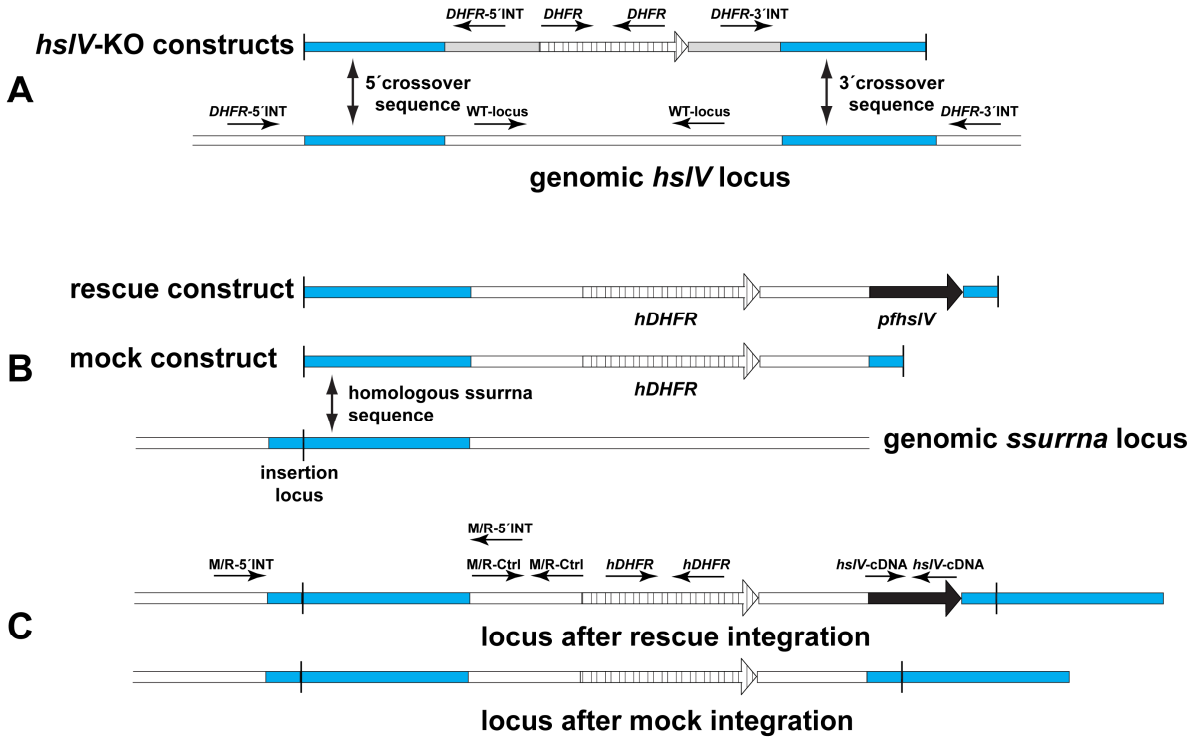

Fig. 4: Generation of *hslV*-KO parasites and rescue/mock parasites.

Horizontal arrows in A and C visualize the primer combinations listed in table 1. Homologous sequences for single/double crossover are marked in dark grey.

(A) Upper row: linearized knockout constructs (first or second knockout), lower row: genomic *hslV* locus. Note that there is only one genomic *hslV* locus, i.e. parasites with a correctly integrated knockout construct at this locus do not contain the *hslV* sequence in their genome.

(B) Upper two rows: linearized rescue and mock constructs, lower row: genomic locus for insertion (*c-ssurrna* or *d-ssurrna* = *small subunit ribosomal RNA* gene of either c- or d-rrna unit).

(C) Rescue and mock constructs after integration into genomic locus via single crossover.

Table 2: Primers for transfection control

Name	Sequence	Expected size of PCR product
Primers for detection of the selectable markers in DNA of transfected parasites		
hdhfr for	5′ - GCATGGTTCGCTAAACTG – 3′	528bp
hdhfr rev	5′ - AATGCCTTTCTCCTCCTG – 3′	
tgdhfr for	5′ - AGAGGGGCATCGGCATCA – 3′	543bp
tgdhfr rev	5′ - TTGAAAGAATGTCATCTC – 3′	
Primers for detection of correct integration of knockout constructs		
hdhfr-5′Int for	5′ - GTTTATATGTGTGGATGTGTTTAC – 3′	837bp
hdhfr-5′Int rev	5′ - CTCGAAAAGAATTAAGCTGG – 3′	
hdhfr-3′Int for	5′ - TGATTCATAAATAGTTGGACTTG – 3′	909bp
hdhfr-3′Int rev	5′ - CCGTTGCATATTGGTGCTA – 3′	
tgdhfr-5′Int for	5′ - GTTTATATGTGTGGATGTGTTTAC – 3′	915bp
tgdhfr-5′Int rev	5′ - AATTATATGTTATTTTATTTCCAC – 3′	
tgdhfr-3′Int for	5′- AAATGTGGGGTAAAAAAGAGTG – 3′	820bp
tgdhfr-3′Int rev	5′- CCGTTGCATATTGGTGCTA – 3′	
Primers for detection of wild type DNA		
WT-locus for	5′- CCACGAAAACAAATAACCACAGC - 3′	1KB
WT-locus rev	5′- CCCGATCCTGTGCCTAAAAC – 3′	
Primers for detection of *pfhslV*-cDNA in rescue-transfected parasites		
pfhslV-cDNA for	5′- GGATCACAAAAATCAATAACC – 3′	696bp
pfhslV-cDNA rev	5′- CTGACATCCTCTTGATTAG – 3′	
Primers for detection of additional mock/rescue specific DNA sequences		
M/R-Ctrl for	5′- CTTGGAGCGAACGACCTAC – 3′	586bp
M/R-Ctrl rev	5′- CGGAAGCATAAAGTGTAAAGC – 3′	
Primers for detection of integrated mock/rescue constructs		
M/R-5′Int for	5′- TTTGGATATTTTCATATATG – 3′	2.1KB
M/R-5′Int rev	5′- TTTCCCAGTCACGACGTTG – 3′	

5.4.2 PCR analysis of genomic *hslV* locus in WT and transfected parasites

All PCRs were done in a 50µl reaction volume containing the following components:

5µl 10x PCR Buffer (Qiagen)

10µl 5x Q-Solution (Qiagen)

3µl 25mM MgCl2 (Qiagen)

2µl dNTP mix (5mM each)

1µl 10mM Forward Primer

1µl 10mM Reverse Primer

2.5µl Taq DNA polymerase (Qiagen)

20-200ng template DNA

Water (LiChrosolv®) up to 50µl

5.4.3 Standard thermocycler settings

(used with all primer combinations except mock/rescue integration-specific primers)

95°C - 2min, (95°C - 30s, 55°C - 30s, 72°C - 60s, 30 cycles), 72°C 7min

5.4.4 Thermocycler settings for mock/rescue integration-specific primers

95°C – 2min

(95°C – 30s, 50°C – 30s, 72°C – 150s, 20 cycles)

(95°C – 30s, 50°C – 30s, 72°C – 150s + 1s time increment, 25 cycles)

72°C – 7min

All PCRs were validated for a “Primus 96 advanced” thermocycler from Peqlab. Other thermocyclers were used on occasions. Every PCR included positive and negative control samples.

5.4.5 Sequencing of PCR products

To confirm their identity, all the above-mentioned PCR products were sequenced as described in section 5.1.5. Sequences were confirmed at least once for every transfection and cloning experiment.

5.4.6 Preparation of parasite protein extracts

Blood, containing the parasites, was obtained as described in section 5.3.4. and spun down (8min, 200g, RT). The erythrocyte pellet was mixed with an equal amount of PBS. Two volumes of a 0.15% saponin in PBS solution were added and erythrocytes were allowed to lyse for 5min at room temperature. Parasites were spun down (1,500g, 15min, 4°C), washed 3 times with 1ml ice-cold PBS (7,500g, 5min, 4°C), and dissolved in a suitable amount of Bäuerle buffer (20mM HEPES, 350mM NaCl, 1mM $MgCl_2$, 0.5mM EDTA, 0.1mM EGTA, 20% Glycerol (v/v), 1% Igepal CA-630, 1 tablet protease inhibitor cocktail per 50ml final volume, stored at -20°C). Protein extracts were stored at -20°C.

5.4.7 Western blotting

For Western blotting parasite protein extracts were spun down (17,000g, 10min, 4°C), and the supernatant was mixed with SDS loading buffer (filtered, aqueous solution containing 125mM Tris pH 6.8, 6% SDS, 20% glycerol, 0.2% bromophenol blue, 10% mercaptoethanol) to a final loading-buffer concentration of 1x. Samples were subsequently separated on a 12% SDS gel using the following gel and buffer mixtures:

Stacking gel: 17% acryl/bis-acryl-amide (30%), 0.1875M Tris (pH6.8), 0.1% SDS, 0.1% ammonium persulphate, 0.1% TEMED

Resolving gel: 40% acryl/bis-acryl-amide (30%), 0.375M Tris (pH 8.8), 0.1% SDS, 0.1% ammonium persulphate, 0.04% TEMED

SDS running buffer: 250mM Tris, 1% SDS, pH8.3

Proteins were blotted in semidry blotting buffer (48mM Tris, 39mM glycine, 0.037% SDS, 20% methanol pH 9.2) onto a nitrocellulose membrane (Bio-Rad, Art. No. 162-0115) by applying a current of $1mA/cm_2$ for 60min.

PbHslV (ClpQ) was visualized using a PfHslV-antiserum, diluted 1:2,000 (Mordmüller et al. 2006) as primary and “anti-rabbit IgG, HRP-linked Antibody”, diluted 1:2,000 (Cell Signaling Technology) as secondary antibody. Proteins were visualized on a Chemi-Smart 5000 imaging system (Peqlab, Erlangen, Germany) using LumiGLO® chemiluminescence detection reagents (Cell Signaling Technology).

To verify binding of all samples to the membrane, some blots were stripped and reprobed with an antibody against a proteasomal α-subunit (mAb MCP231 from anti-proteasome α -subunit sampler pack, Biomol, Hamburg, Germany). Stripping was

done by incubation in stripping buffer (62.5mM Tris-HCl, pH 6.7; 2% SDS; 100mM β-mercaptoethanol) for 30min at 50ºC. Detection of reprobed blots was done as described above, using “anti-mouse IgG, HRP-linked Antibody” (Cell Signaling Technology).

5.4.8 Bio-Plex cytokine and chemokine assays

Levels of selected cytokines and chemokines were determined in sera of three WT and three *hslV*-KO-infected CD1^{TM} mice at the following time points:
1 day prior to infection (baseline) and 3, 6 or 9 days after infection.
Mice were infected with 1000 parasites as described for the parasite growth assays.
Samples were stored at -20°C and then analyzed on a Bio-Plex® 200 system (Bio-Rad) using a magnetic bead Bio-Plex Express Assay (Bio-Rad) with the following cytokines: IL-1α, IL-1β, IL-6, IL-12p40, IL-12p70, IFN-γ and MIP-1α.
In a second experiment using 6 mice per group, the following cyto- and chemokines were additionally measured: IL-10, MIP-1β, Eotaxin, KC, MCP-1, Rantes, LIF, MIG, TNF-α and MIP-2.

5.5 Further phenotyping methods

5.5.1 Spleen-weight determination

For a number of animals the spleen weight/body mass ratio was determined at time of death. For this purpose, spleens were dissected and spleens and animals weighed on a precision scale.

5.5.2 Reticulocyte counts

To determine a possible influence of the *hslV*-KO parasites on hematopoiesis, the ratio of polychromatic reticulocytes was determined on Giemsa-stained blood smears from WT and *hslV*-KO-infected CD1^{TM} mice from three to six days post infection (staining protocol see section 5.3.3).

5.5.3 Cellular imaging

To investigate possible differences in mitochondrial shape or size between knockout and wild type parasites, unfixed parasites were stained with the mitochondrial stain MitoTracker Red® and a DNA counterstain (Hoechst 33342), and subsequently assessed by flow cytometry (using a FACSCanto II cytometer) and fluorescence microscopy (using a Leica DMLB microscope).

Parasites were stained for 30 min using the following dye concentrations:

Hoechst 33342: 10µg/ml (FACS) and 0.033µg/ml (fluorescent microscopy)

MitoTracker Red®: 0.5µM (FACS) and 2nM (fluorescent microscopy)

5.5.4 Statistics

Significance levels for differences in growth rates and reticulocyte counts were calculated by comparing the AUCs (areas under the curve) for WT and *hslV*-KO parasitemia / reticulocyte courses using Student's two-tailed t-test. AUC values were determined by trapezoidal rule. For growth rates AUCs were obtained from the infection time point until either all WT or all *hslV*-KO-infected mice had died. Missing parasitemia values for animals dying prior to this endpoint were set as the last known value (LOCF method). For reticulocyte counts AUCs were obtained for the time frame investigated (three to six days post infection).

Significance levels for survival times were determined by logrank test, since this test is the most commonly used test to compare survival curves (Schoenfeld 1981).

6 LIST OF REAGENTS

Item	Provider	Art.-No.
Acryl/Bis-Acryl-amide (30%)	Sigma-Aldrich, Munich, Germany	A2792-100ML
Ammonium persulphate	Amresco, Ohio, USA	04861-100g
Bromophenol blue	Sigma-Aldrich, Munich, Germany	B0126-25G
Disodium hydrogen phosphate dihydrate	VWR International GmbH, Darmstadt, Germany	28.029.292
Ethylenediaminetetraacetic acid (EDTA)	Merck, Darmstadt, Germany	100944
Ethylenediaminetetraacetic acid (EDTA) calcium disodium salt	Sigma-Aldrich, Munich, Germany	ED25C-100G
Ethylene glycol tetraacetic acid (EGTA)	Sigma-Aldrich, Munich, Germany	E3889-100G
Gentamicin, liquid, 50 mg/ml	Invitrogen, Karlsruhe, Germany	15750-037
Giemsa's azure eosin methylene blue solution	Merck, Darmstadt, Germany	1.09204.1000
Foetal Bovine Serum GOLD	PAA Laboratories, Cölbe, Germany	A15-151
Glycerol, purum, anhydrous	Sigma-Aldrich, Munich, Germany	49780-1L
Glycine	Roth, Karlsruhe, Germany	3908.2
L-Glutamine solution, 200 mM	Sigma-Aldrich, Munich, Germany	G7513

Item	Provider	Art.-No.
Hayem´s reagent	Merck, Darmstadt, Germany	1.09260
HEPES solution, 1M	Sigma-Aldrich, Munich, Germany	H0887
Histodenz™ powder	Sigma-Aldrich, Munich, Germany	D-2158
Hoechst 33342	Invitrogen, Karlsruhe, Germany	H1399-100mg
IGEPAL® CA-630	Sigma-Aldrich, Munich, Germany	13021
LiChrosolv®, Water for chromatography	Merck, Darmstadt, Germany	1.15333.2500
Liquemin N5000	Roche, Grenzach, Germany	PZN 3441118
β-Mercaptoethanol	Sigma-Aldrich, Munich, Germany	63689
Methanol	Merck, Darmstadt, Germany	1.06009.2511
MitoTracker Red® CMX Ros	Invitrogen, Karlsruhe, Germany	M7512
Potassium chloride	Merck, Darmstadt, Germany	104936
Potassium dihydrogen phosphate	Merck, Darmstadt, Germany	30.06.06
Protease Inhibitor Cocktail Tablets	Roche, Grenzach, Germany	11697498001
Pyrimethamine powder	Sigma-Aldrich, Munich, Germany	P7771

Item	Provider	Art.-No.
RPMI-1640 Medium with NaHCO3	Sigma-Aldrich, Munich, Germany	R0883
SDS ultrapure	Roth, Karlsruhe, Germany	2326.2
TEMED	Roth, Karlsruhe, Germany	2367.3
Trizma® Base	Sigma-Aldrich, Munich, Germany	T1503
WR99210	JACOBUS PHARMACEUTICAL COMPANY, INC., Princeton, NJ, USA	N/A

7 RESULTS

7.1 *hslV*-KO parasites are viable in the murine host

To assess the essentiality as well as possible functions of *hslV*, *hslV*-deficient *P. berghei*-parasites were generated. The knockout was achieved by transfection of two different knockout constructs, containing *hdhfr* as selectable marker sequence for the first knockout and the *tgdhfr* selectable marker sequence for the second knockout. The second knockout, containing *tgdhfr* as a selectable marker was generated to facilitate the cotransfection of a *hdhfr*-containing rescue construct, by selection of the *hslV*-KO-transfected parasite population with pyrimethamine and the rescue-transfected parasite population with the antimalarial WR99210 as described in section 5.3.6.

Following the transfection procedure, parasites were cloned, which led to six independent knockout clones with correctly integrated *hdhfr* construct for the first knockout and two clones with correctly integrated *tgdhfr* construct for the second knockout. Correct integration of the transfected sequences was assessed by PCR using the primers provided in the first three sections of table 2 (section 5.4.1). The location of these primers is given in fig. 4. In case of successful transfection the primers for detection of the used selectable marker sequence (*tgdhfr* or *hdhfr*) should yield a PCR product of ca. 550bp length, whereas the 5´- and 3´-integration-specific primers for the knockout constructs should yield PCR products of ca. 900bp length. The WT locus-specific primers should yield a 1KB long PCR product only in wild type parasites. All PCRs resulted in products of the expected sizes. PCR products were only detectable using DNA extracts containing the sequences targeted by the respective primers (for a representative PCR result see fig. 5).

The identity of all PCR products was additionally confirmed by sequencing following each transfection or cloning experiment.

Obtained results, as depicted in fig. 5, demonstrate that the transfected *hslV*-KO sequence integrated into the *hslV* locus and that no residual WT parasites were present in the clonal parasite populations.

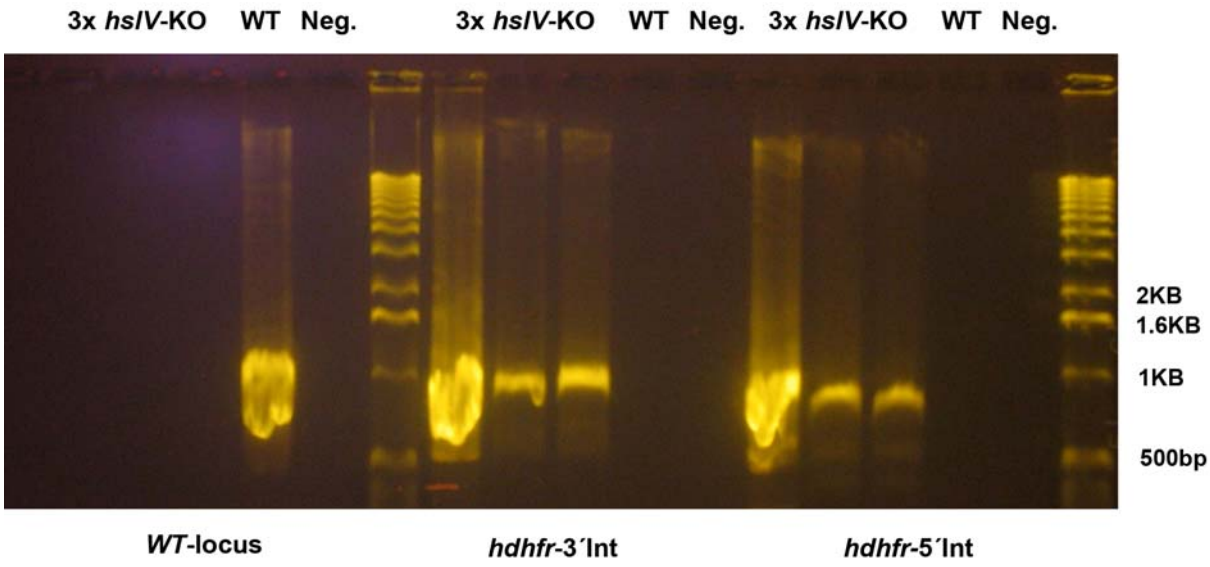

Fig. 5: Agarose gel showing PCR results that confirmed correct integration of the first knockout construct (containing *hdhfr* as a selectable marker) in three parasite clones. Note that the *hslV*-WT-locus is no longer detectable in the knockout parasites.

Upper labels indicate the used template DNA (Neg. = negative control), lower labels refer to the used primer sets. *hdhfr*-5´Int and *hdhfr* 3´Int primers span the integration site at the 5´UTR and 3´UTR of the *hslV* locus. In case of correct integration the PCR yields integration-specific PCR products of 837bp (5´UTR) and 909bp (3´UTR) length respectively, whereas no PCR product is expected in untransfected WT parasites. The WT locus-specific PCR in contrast targets the *hslV* sequence, which is replaced by the integrating DNA during double crossover, therefore amplification of the 1KB long PCR product is only expected in WT parasites, but not in *hslV*-KO parasites. Results show that all PCR products have the expected sizes and do occur in the expected parasite lines, i.e. integration-specific PCR products occur only in *hslV*-KO parasites and WT-locus PCR products occur only in WT parasites.

7.2 *hslV*-KO parasites do not express ClpQ

The *hslV* expression level was determined by Western blot analysis of parasite protein extracts of *hslV*-KO and WT parasites using an α-PfHslV-antiserum (Mordmüller et al. 2006). Cross reactivity of the α- PfHslV serum with PbHslV was initially confirmed by comparing blotting results of *P. falciparum* and *P. berghei* protein extracts. On Western blot HslV appears as two distinctive bands at 18 and 23 kDA (corresponding to the processed (active) and unprocessed form of the protease), which are always detectable in unsynchronized WT parasites. As expected, cloned knockout parasites showed no residual *hslV* expression (see fig. 6).

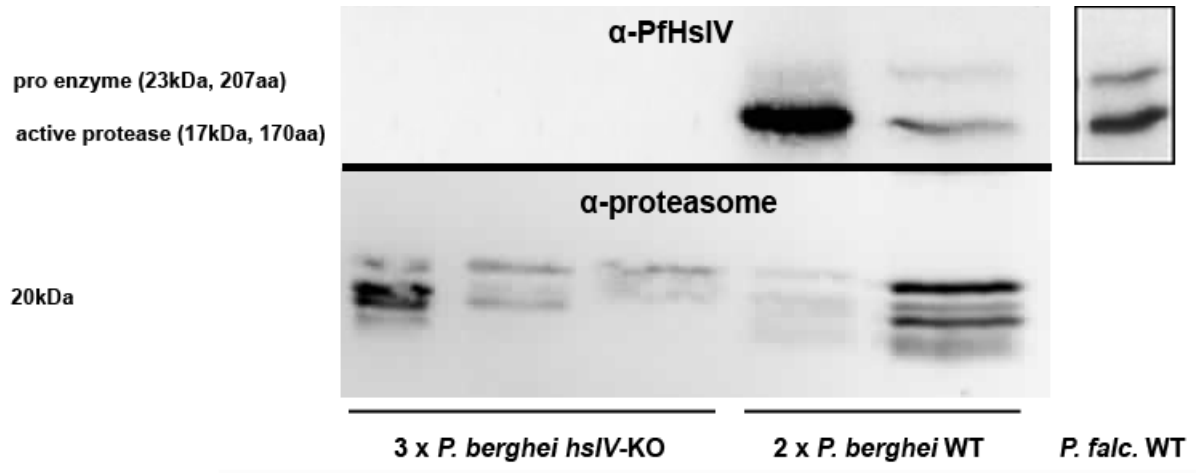

Fig. 6: Blotted extracts of *hslV*-KO and WT parasites.

Upper panel:
Three *P. berghei hslV*-KO and two *P. berghei* WT extracts probed with anti-PfHslV. The right picture shows a blotted *P. falciparum* WT extract for comparison [picture derived from (Mordmüller et al. 2006)]. The two bands correspond to the unprocessed form of PbHslV (23kDa) and the mature protease (17kDa).

Lower panel (loading control):
Same blot stripped and reprobed with mAb MCP231, an antibody recognizing the α-subunit of the proteasome, confirming the presence of sample in all lanes.

7.3 PbHslV (ClpQ) deletion leads to growth retardation of asexual parasite blood stages and alters the survival time of the host

To assess the fitness of the ClpQ-deficient parasites, mice of three different strains were intravenously infected with 1000 WT- or *hslV*-KO-parasites, respectively, followed by daily parasitemia counts on Giemsa stained thin blood smears. The investigation of growth rates in three different mouse strains was motivated by the finding of a significantly slower growth rate of the *hslV*-KO-parasites in CD1^{TM} (outbred) mice. To further evaluate the importance of this finding the experiment was

repeated with the two immunologically distinct inbred mouse strains C57BL/6 and BALB/c. C57BL/6, a cerebral malaria susceptible mouse strain, is believed to mount a Th1 dominated immune response, whereas the cerebral malaria resistant BALB/c mouse seems to mount a more Th2 dominated immune response (Mills et al. 2000).

These *in vivo* parasite growth assays revealed a significantly slower growth (i.e. parasitemia development over time) of ClpQ-deficient parasites, compared to WT parasites. The observed growth retardation was significant for all three mouse strains used (CD1^{TM} mice, $p < 0.001$, C57BL/6 mice, $p = 0.01$, and in BALB/c mice, $p < 0.001$; see fig. 7). Assays in CD1^{TM} mice were conducted with parasites of three different knockout clones and growth retardation was evident for parasites of all three clones.

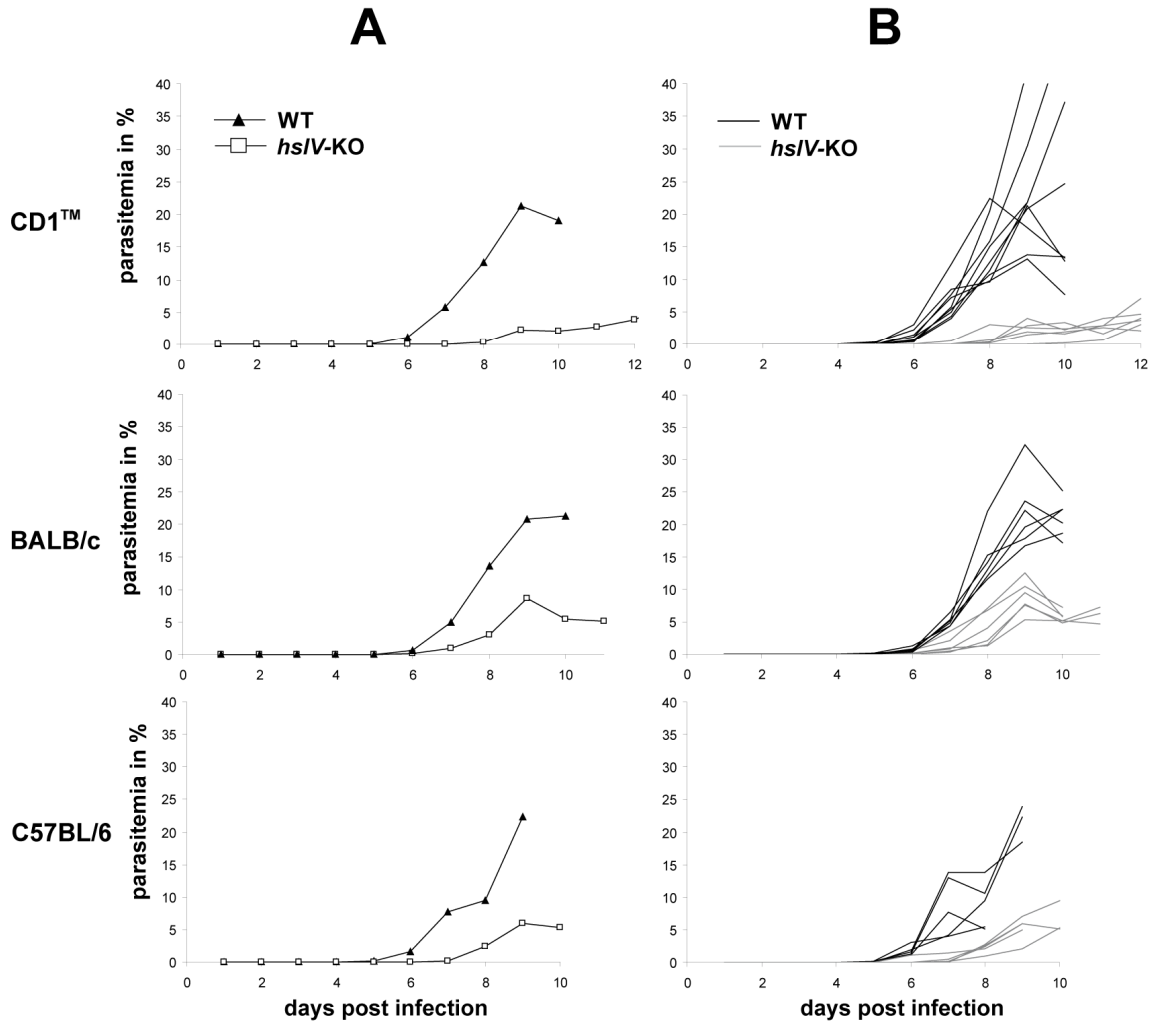

Fig. 7: Course of parasitemia in *hslV*-KO- and WT-infected animals in different mouse strains.

(A) Median parasitemia of 9 WT and 6 *hslV*-KO-infected animals (CD1^{TM} mice), 6 mice per parasite line (BALB/c), and 5 mice per parasite line (C57BL/6).

(B) Parasitemia course in the same mice per animal. Discontinued lines prior to end of time axis represent animal deaths.

Besides its effect on growth, PbHslV deletion had a significant impact on survival times of infected mice: CD1^{TM} and C57BL/6 mice, infected with *hslV*-KO parasites, survived significantly longer than WT-infected animals, whereas *hslV*-KO-infected BALB/c mice had a shorter survival time than WT-infected BALB/c (see fig. 8).

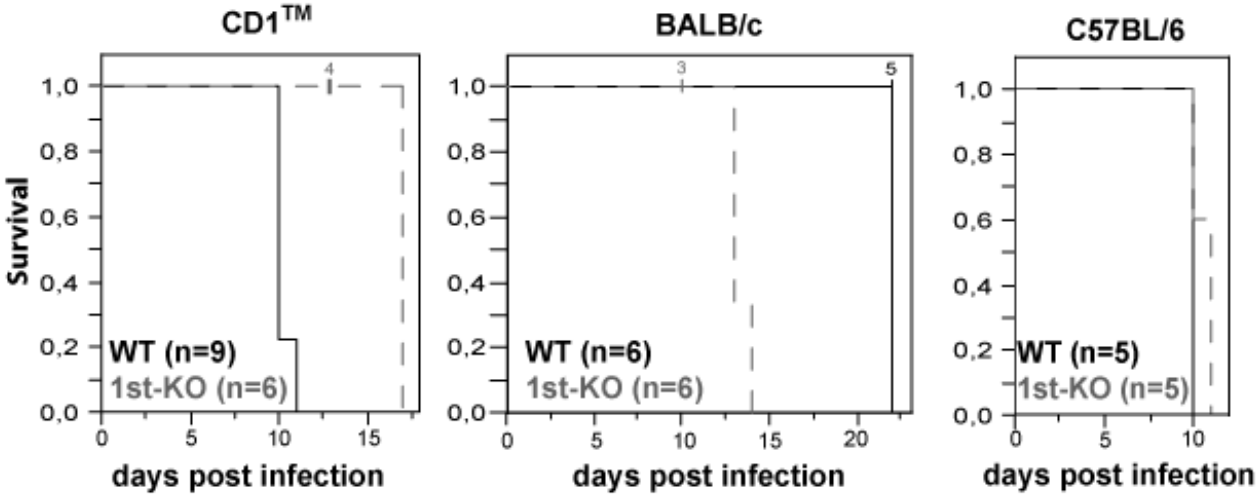

Fig. 8: Kaplan-Meier plots depicting survival times of three different mouse strains following infection with *hslV*-KO parasites (first knockout) or WT parasites.

Note the reverse correlation of *hslV*-KO genotype and survival times in BALB/c mice compared to CD1^{TM} and C57BL/6 mice. n = total number of animals per curve. Small vertical lines indicate censored animals (death not associated with malaria), digits represent the number of censored animals.

Differences in survival time were significant in all comparisons (logrank test, $p < 0.001$ for CD1^{TM}, $p < 0.01$ for BALB/c, and $p < 0.05$ for C57BL/6 mice).

7.4 Parasite growth retardation can be rescued by cotransfection of *pfhslV* into a separate genomic locus

To show that *hslV* itself caused the observed growth retardation, *hslV*-KO parasites were cotransfected with *pfhslV*, i.e. a single crossover construct containing the *P. falciparum* cDNA sequence was transfected. This vector was designed to integrate into either the *c*- or *d-ssurrna* gene. To control for phenotypic effects caused by this integration event or by the selective drug treatment, a mock-transfected parasite line was generated. Mock parasites were transfected with a modified rescue construct lacking the *pfhslV*-cDNA sequence. DNA extracts of rescue- and mock-transfected parasites were analyzed by PCR using all primers listed in table 2 (section 5.4.1). PCR analyses using these primers allow to determine the genotype of the different parasite lines (WT, *hslV*-KO, rescue and mock) by comparison of the resulting PCR products, as shown in fig. 4. Primer pairs targeting the selectable marker sequences *hdhfr* and *tgdhfr* only yielded PCR products in transfected parasite lines containing those sequences, integration-specific primer pairs only yielded PCR products in case of successful 3´- or 5´-integration of the transfected DNA into the targeted locus. WT-locus primers only yielded a PCR product in WT parasites with an intact *hslV* locus, whereas in knockout parasites no product was detected. The *pfhslV*-cDNA primers only amplified a PCR product in rescue-transfected parasites, whereas the M/R-control primers targeted a sequence present within both the mock and the rescue vector.

PCR results showed that both mock and rescue constructs integrated correctly into at least one of the genomic *c-ssurrna* or *d-ssurrna* loci and all PCR products had the expected sizes, i.e. ca. 550bp for the selectable marker sequences and for the M/R-control-PCR, 700bp for the *hslV*-cDNA sequence, 1KB for the WT-specific PCR, and 2.1KB for the mock/rescue integration-specific PCR (see fig. 9 for a representative PCR result).

The identity of all PCR products was additionally confirmed by sequencing following each transfection or cloning experiment.

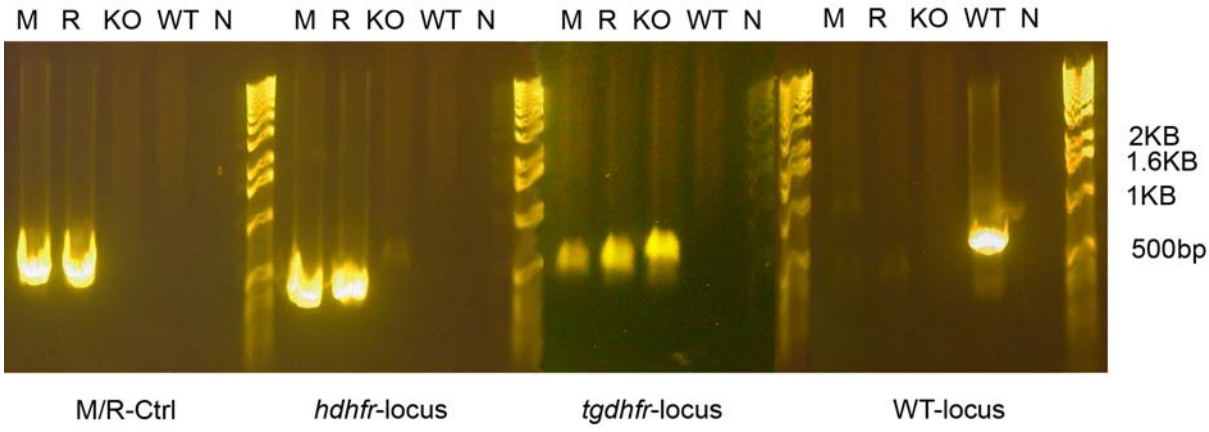

Fig. 9: Agarose gel showing PCR results for the transfection control of cloned parasite lines.

Upper labels indicate the used template DNA (M = Mock, R = Rescue, KO = *tgdhfr*-KO, WT = wild type, N = negative control), lower labels refer to the used primer sets.

The results confirmed the correct integration of transfection constructs. The M/R-specific sequence and the selectable marker for the mock and rescue parasites (*hdhfr*) are only detectable in DNA extracts of mock and rescue parasites. The selectable marker for the knockout, which even is present after mock or rescue cotransfection, is detectable in all transfected parasite lines, but not in WT parasites, whereas the sequence of the genomic *hslV*-locus is only detectable in WT parasite extracts.

Western blot analyses of protein extracts of cloned mock and rescue parasites confirmed restored expression of ClpQ in its processed (active) and unprocessed form in the rescue parasites and lacking ClpQ expression in the mock parasites (see fig. 10).

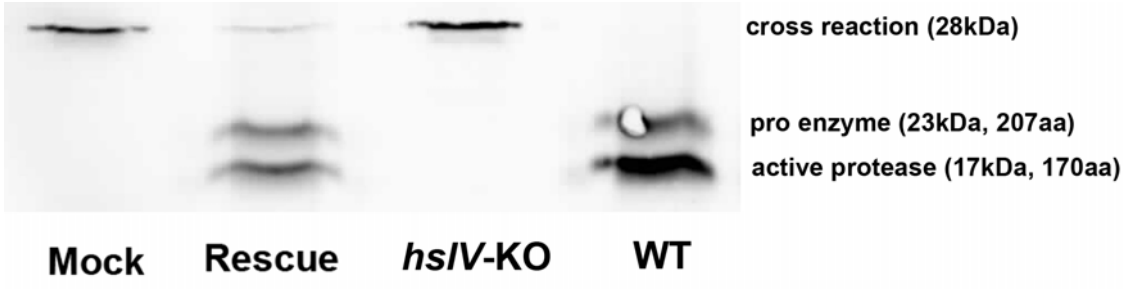

Fig. 10: Blotted extracts of different parasite lines probed with anti-PfHslV.

Upper bands represent a 28kDa-cross-reaction, which is occasionally detected by the PfHslV-antiserum in WT as well as in *hslV*-KO parasites.

In mice, treated with the antimalarial drug WR99210, growth rates of rescue-transfected parasites were significantly higher than those of mock-transfected parasites ($p < 0.001$), comparable to the relation of growth rates of WT and *hslV*-KO parasites in untreated mice (see fig. 11). The WR99210-treatment was necessary to prevent reversion of rescue and mock lines to the parental genotype (*hslV*-KO), since the cotransfected rescue and mock constructs, in contrast to the stably integrated knockout construct, were integrated by single-crossover and could therefore be lost again in the absence of drug pressure (Thathy and Ménard 2002).

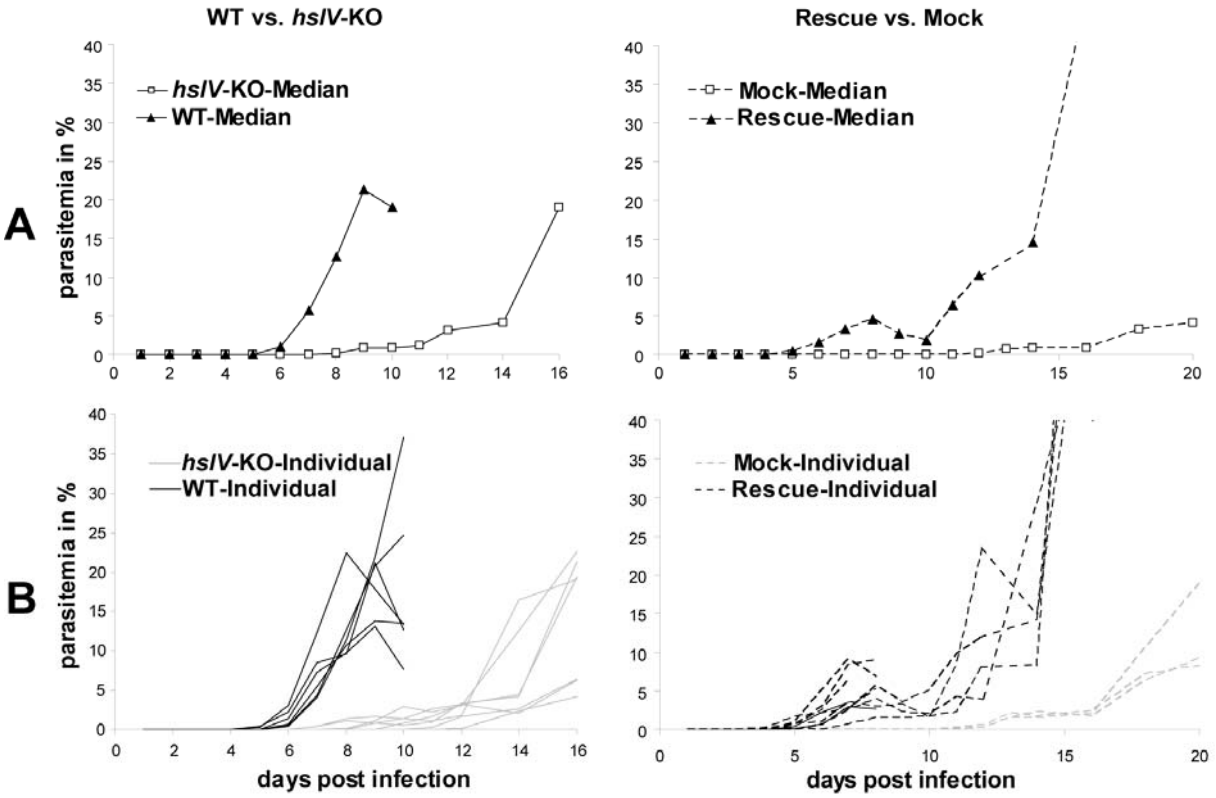

Fig. 11: Growth rates of WT and *hslV*-KO (left panel) vs. rescue- and mock-transfected parasites (right panel).

Growth rates were determined in CD1^{TM} mice. A: median parasitemia values for 6 - 10 animals per curve, B: individual parasitemia values for those animals (note that out of 6 mock-infected mice only 3 did develop a detectable parasitemia). *hslV*-KO growth rates differ from fig. 7 since those data refer to first knockout line transfected with *hdhfr* and here to the second line transfected with *tgdhfr*.

Survival times of *hslV*-KO and mock-infected mice were significantly prolonged compared to the survival times of WT- or rescue-infected mice, respectively (see fig. 12).

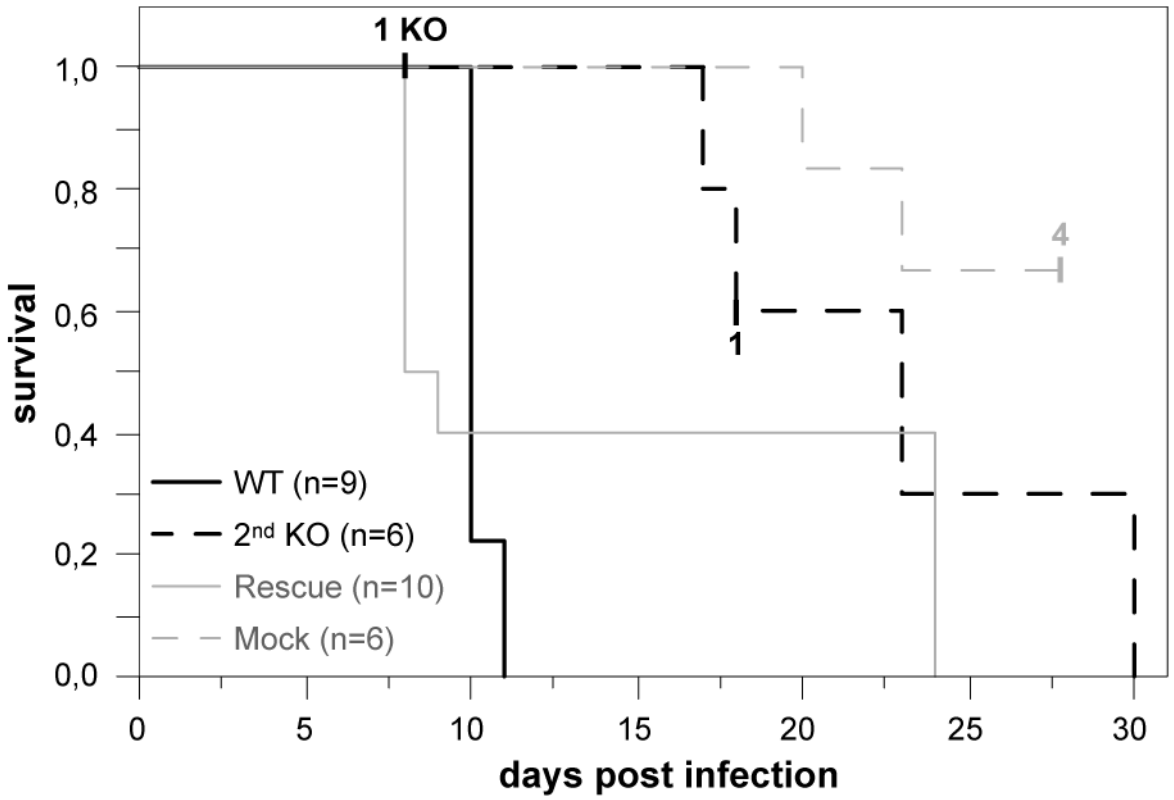

Fig. 12: Kaplan-Meier plot depicting survival times of CD1^{TM} mice infected with four different parasite lines. n = total number of animals per curve. Small vertical lines indicate censored animals (death not associated with malaria), digits represent the number of censored animals. All alterations in survival times were significant (logrank test, $p < 0.001$ for WT vs. *hslV*-KO and $p < 0.05$ for rescue vs. mock).

7.5 Similar growth of WT and *hslV*-KO parasites in MyD88-KO mice.

To test a potential involvement of TLR-mediated processes in the observed growth retardation, the growth assays were repeated using MyD88-KO mice on the background of C57BL/6. Since MyD88 is a downstream mediator molecule of all murine TLRs except TLR 3, MyD88-deficient mice can be regarded as a model for TLR non-functionality. In MyD88-deficient mice *hslV*-KO parasites grew at a similar rate as WT parasites, and differences in growth were no longer significant ($p = 0.1$). Median survival time of *hslV*-KO-infected MyD88-KO mice was two days shorter compared to WT-infected MyD88-KO mice, and this observation was significant ($p < 0.01$), (see fig. 13). Irrespective of the infecting parasite line, MyD88-KO mice survived about 10 days longer than intact C57BL/6.

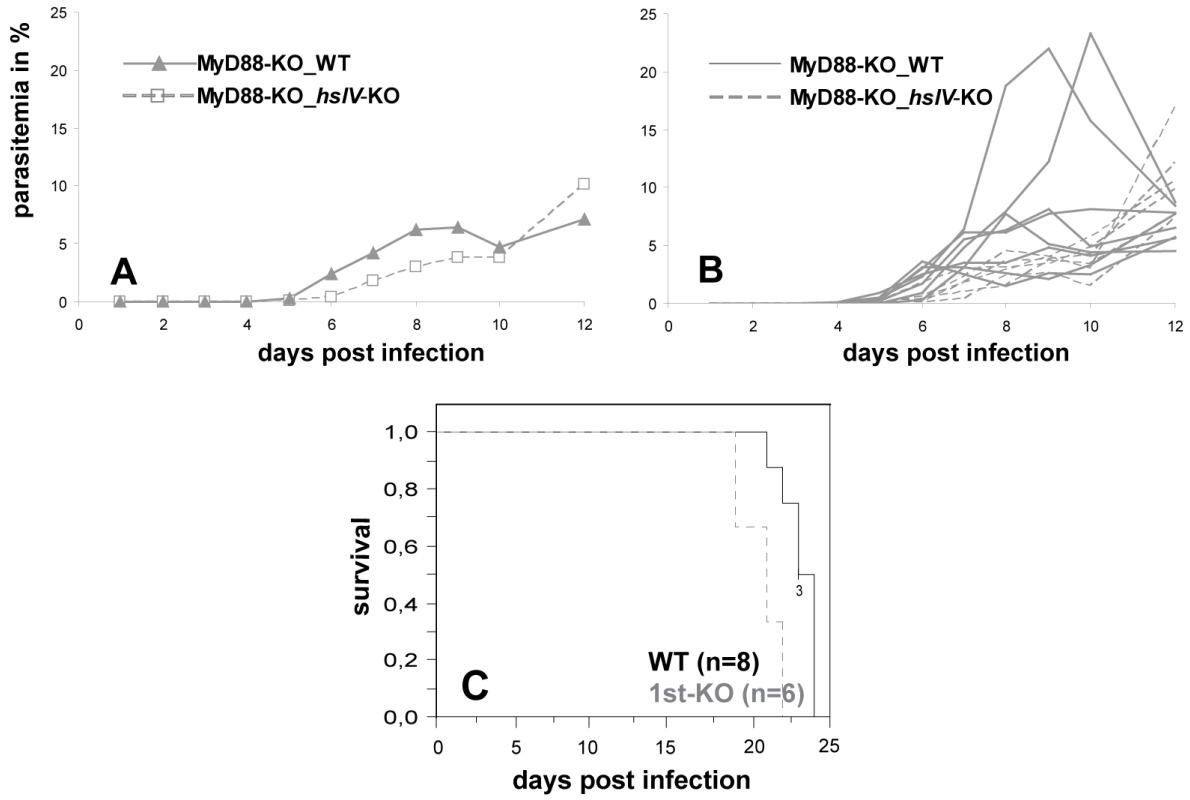

Fig. 13: Course of parasitemia and survival rates of *hslV*-KO and WT-infected MyD88-KO mice (genetic background C57BL/6).

(A) Median parasitemia of eight WT and six *hslV*-KO (first knockout) infected MyD88-KO mice.

(B) Individual parasitemia courses for the animals from A.

(C) Kaplan-Meier plot depicting survival times of MyD88-KO mice following infection with *hslV*-KO parasites - first knockout (interrupted lines) and WT parasites (continuous lines). Small vertical lines indicate censored animals (death not associated with malaria), digits represent the number of censored animals.

7.6 Results of first physiological and immunological investigations

7.6.1 Intact C57BL/6 mice infected with *hslV*-KO parasites have an increased spleen weight.

It is known that *P. berghei*-infected mice develop a considerable splenomegaly during the course of the disease, which is partly caused by proliferation of the red pulp and even more by proliferation of the splenic lymphoid tissue, the white pulp (Eling et al. 1977, Freeman and Parish 1978). Therefore, post-mortal spleen weight of *hslV*-KO- and WT-infected animals was determined as a first indicator of immunologic responses of the host's immune system.

Post-mortal spleen weight determination in three WT-infected and five *hslV*-KO-infected C57BL/6 mice revealed a significantly higher spleen weight/body weight ratio for the knockout animals, p = 0.003, as calculated by t-test (see fig. 14).

Spleen-weight measurements in CD1^{TM} and BALB/c mice showed no differences between WT- and *hslV*-KO-infected animals.

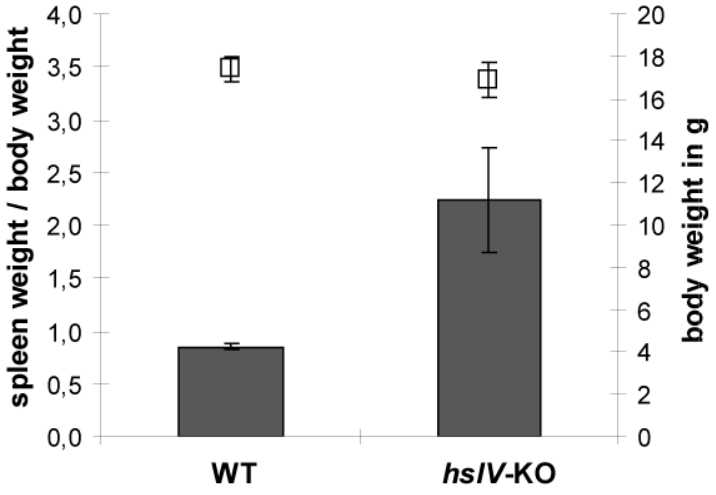

Fig. 14: Post-mortal spleen weight in C57BL/6 (5 *hslV*-KO and 3 WT-infected mice).

Grey bars represent mean spleen weight as percent of body weight, small squares represent mean bodyweight of the animals (error bars indicate double standard deviations). Sampling time points: WT 3x 9 days post infection, *hslV*-KO = 2x 9 and 3x 10 days post infection.

7.6.2 White blood cell counts do not differ significantly between *hslV*-KO and WT parasites.

To investigate the host's immune response further for possible changes caused by the altered genotype of the knockout parasites, white blood cell (WBC) populations in peripheral blood of *hslV*-KO- and WT-infected animals were measured at three consecutive time points. For WT parasites it was expected to see a drop in peripheral WBC counts at 2-4 days post infection. In own experiments WT- as well as *hslV*-KO-infected mice showed a transient drop in peripheral leukocyte counts at two days post infection. This leucopenia was due to a simultaneous decrease of all WBC populations measured (lymphocytes, monocytes and granulocytes), but there were no apparent differences between WT- and *hslV*-KO-infected animals (see fig. 15).

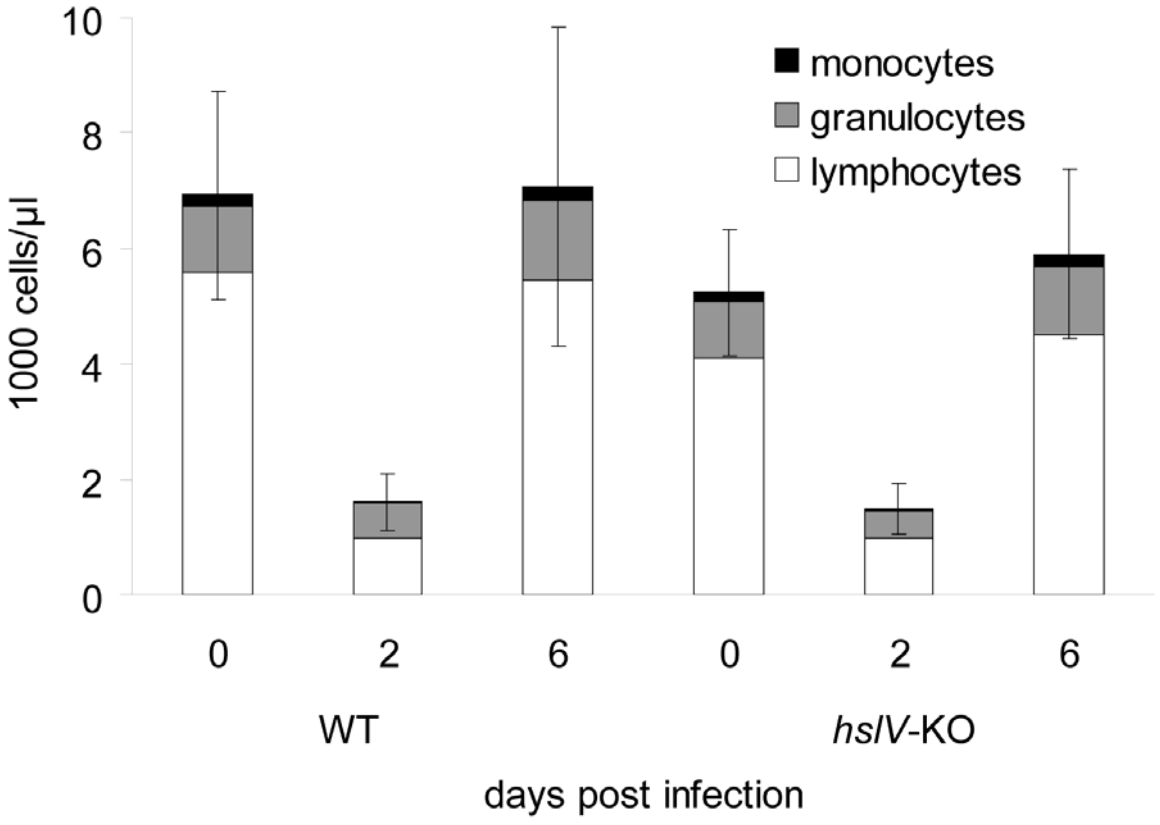

Fig. 15: WBC numbers measured in six WT and twelve *hslV*-KO-infected CD1^{TM} mice prior to infection, and two and six days post infection. Bars and error bars (= 2x standard deviation) represent mean total WBC values, bar sections the fractions of WBCs as indicated in the legend.

7.6.3 Reticulocyte counts do not differ significantly between *hslV*-KO and WT parasites.

In accordance with results of other researchers (Maggio-Price et al. 1985) reticulocyte counts of WT and *hslV*-KO-infected mice approximately doubled between day three and six post infection, but values indicated no differences between *hslV*-KO and WT parasites (see fig. 16).

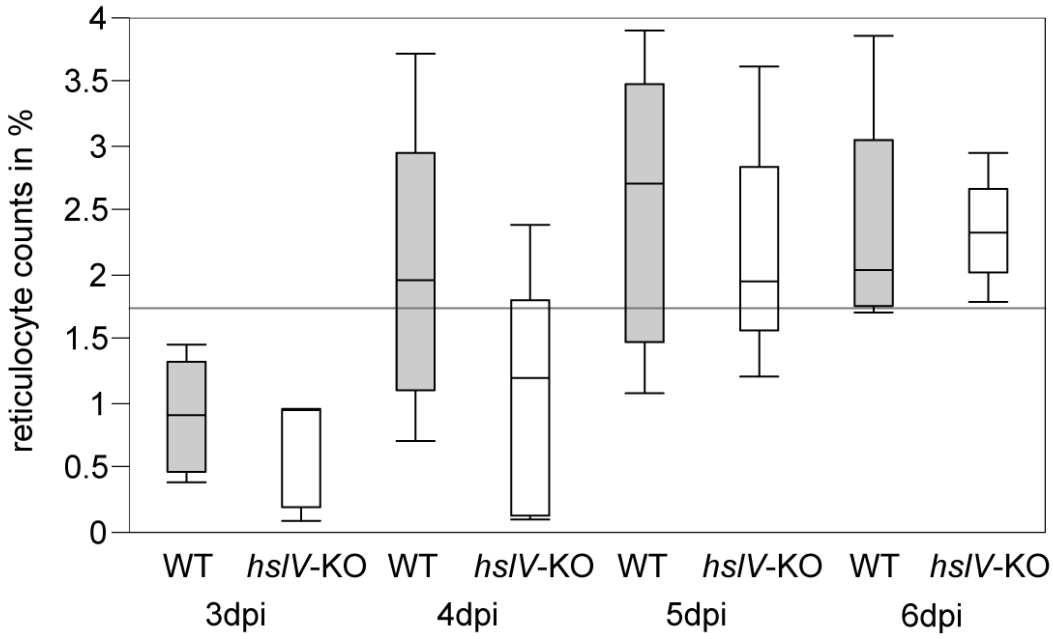

Fig. 16: Reticulocyte counts during the course of WT and *hslV*-KO infections do not differ significantly ($p = 0.29$).

7.6.4 Serum cytokine and chemokine levels do not differ significantly between *hslV*-KO and WT parasites.

To further characterize the immune response of the host, changes in cytokine and chemokine levels were determined in the sera of WT- and *hslV*-KO-infected mice prior to infection and three, six and nine days post infection. As described in the literature, it was expected to see an upregulation of proinflammatory cytokines, such as IFN-γ and TNF-α during early stages of infection (Hanum et al. 2003, Stevenson and Riley 2004). However, own results showed no clear trends of cytokine regulation in the obtained serum samples and no significant differences between WT- and *hslV*-KO-infected animals (see fig. 17).

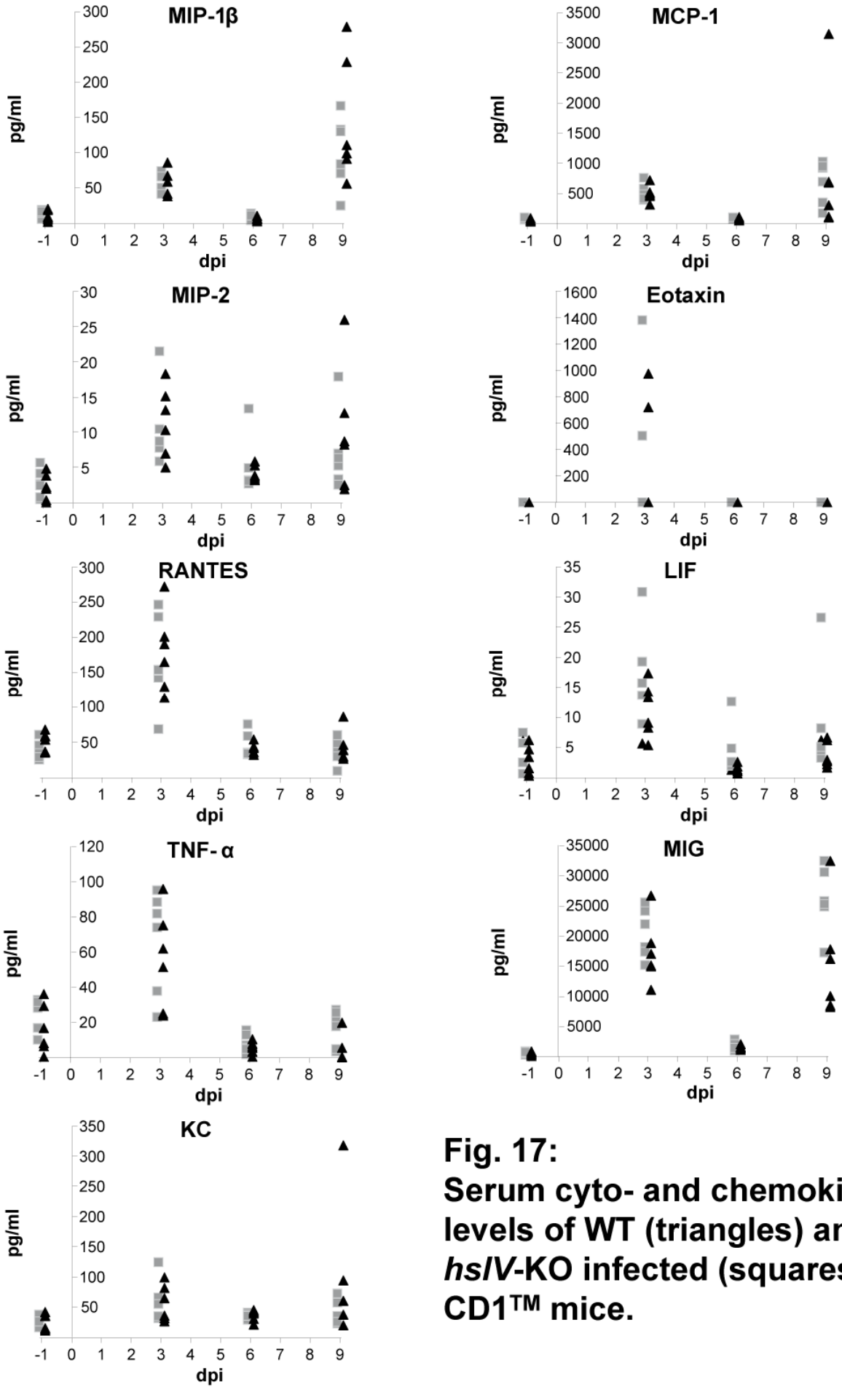

Fig. 17:
Serum cyto- and chemokine levels of WT (triangles) and *hslV*-KO infected (squares) CD1™ mice.

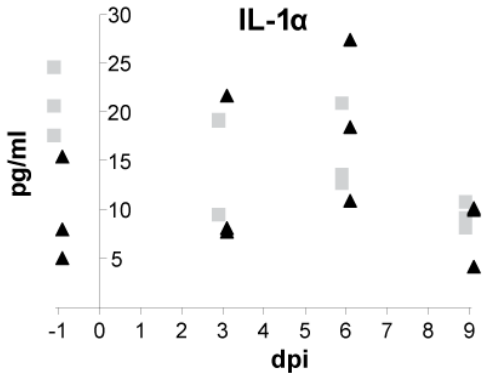
IL-1α
pg/ml
dpi

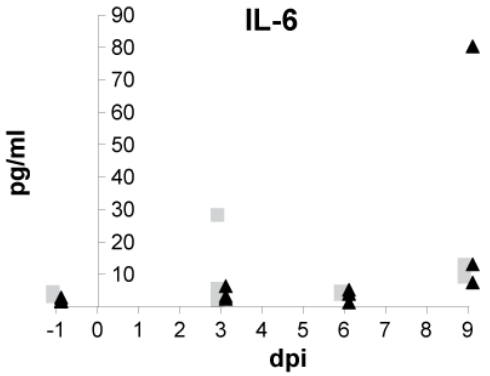
IL-6
pg/ml
dpi

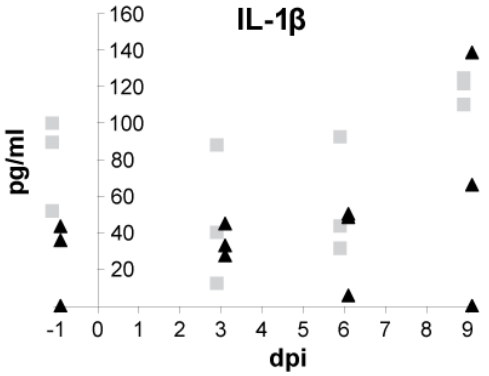
IL-1β
pg/ml
dpi

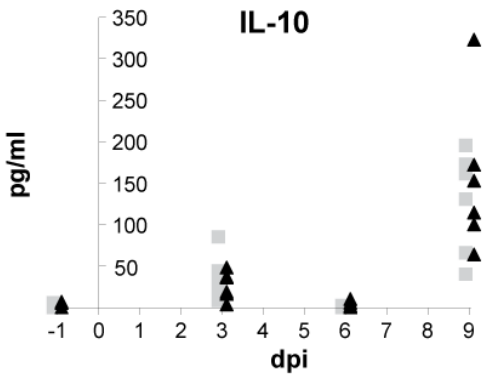
IL-10
pg/ml
dpi

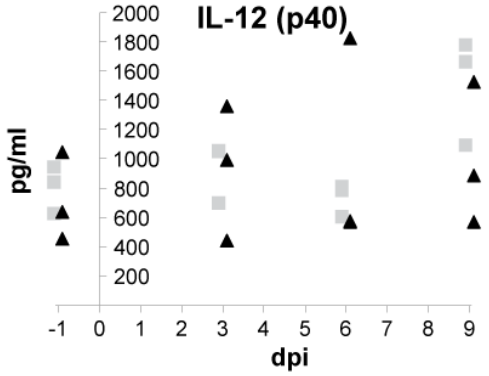
IL-12 (p40)
pg/ml
dpi

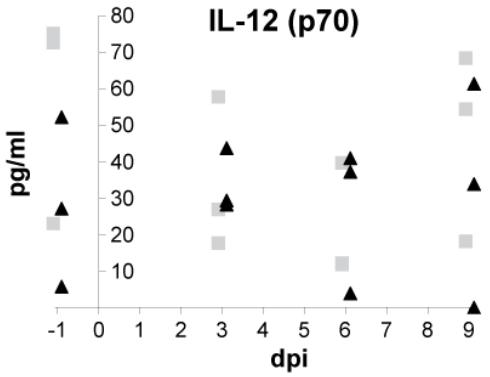
IL-12 (p70)
pg/ml
dpi

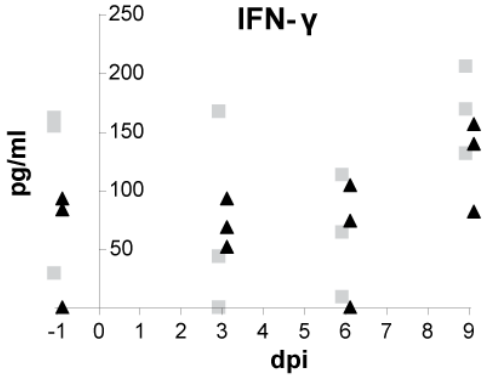
IFN-γ
pg/ml
dpi

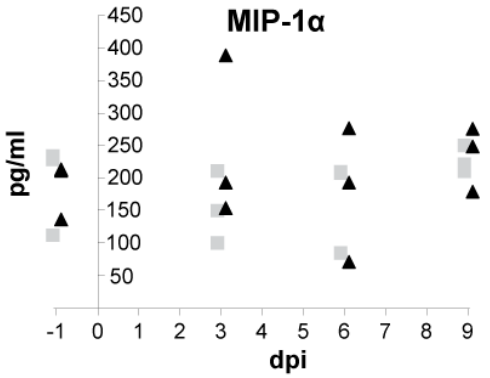
MIP-1α
pg/ml
dpi

7.6.5 Mitochondrial DNA of WT and *hslV*-KO parasites show distinct MitoTracker staining patterns

Since previous experiments showed that *hslV* of *P. falciparum* is located within the mitochondrion (Tschan et al. 2010), the mitochondrial phenotype of WT and *hslV*-KO *P. berghei* parasites was investigated by Mitotracker-staining. MitoTracker Red is a red fluorescing dye that accumulates within the mitochondrion. Here it was used to compare shape and structure of the plasmodial mitochondria between *hslV*-KO and WT parasites. To visualize the nuclei of the parasites, samples were counterstained with the DNA-staining dye Hoechst 33342. Stained *hslV*-KO parasites showed distinct Mitotracker aggregations, which were not evident in WT parasites (see fig. 18). The reason for this altered mitochondrial shape remains to date unclear.

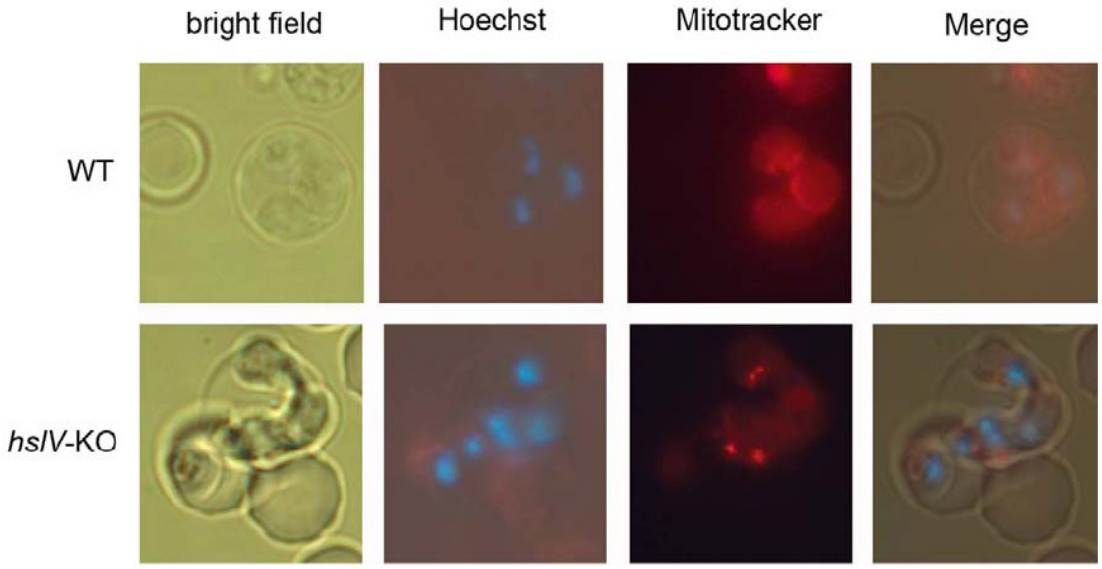

Fig. 18: Mitotracker staining of WT and *hslV*-KO parasites

Attempts to quantify these effects by flow cytometric assessment of MitoTracker stained parasites were not successful due to different parasite stages in mixed blood stage infections.

8 DISCUSSION

8.1 *hslV* deficiency in *P. berghei* leads to the phenotype "retarded growth"

Experiments in this thesis should clarify, whether the threonine peptidase ClpQ of *P. berghei* is essential for the parasite, and if possible, to further characterize its function. To achieve this goal *hslV*-KO parasites were generated. If proven to be essential for the parasite, *hslV* would have been a candidate gene for drug targeting. The fact that the *hslV*-KO parasites were viable, shows that ClpQ is not essential for the development of *P. berghei* in its murine host. Although this finding suggests that *hslV* probably is not suitable as a drug target, the observed phenotype of the knockout parasites still was interesting in view of a functional characterization of ClpQ.

The *in vivo* growth assays showed that *hslV*-deficient *P. berghei* parasites have a distinct phenotype, i.e. significantly reduced growth rates of the asexual blood stages. Growth rates were determined by daily parasitemia counts during controlled WT- and *hslV*-KO-infections. The growth retardation was evident in all three mouse strains investigated (CD1^{TM}, BALB/c and C57BL/6 mice). Observed growth rates for WT parasites in C57BL/6 and BALB/c mice were in accordance with previously published reports (Griffith et al. 2007, Hanum et al. 2003), while for CD1^{TM} mice no comparable data exist.

Rescue transfection of the Plasmodium falciparum *hslV*-cDNA-sequence led to restored expression of both pre-processed and active form of *hslV* (see fig. 10). This was expected due to the high degree of homology between different plasmodial species (Mordmüller et al. 2006) and indicates that the rescue parasites express a functional form of ClpQ.

The reversal of the observed growth retardation in rescue-transfected parasites, caused by the insertion of *hslV* into a completely different genomic locus, demonstrated that the protease itself is responsible for this phenotype. The insertion of transfection constructs into the *c- or dssurrna* locus has previously been shown not to influence parasite growth rates (Franke-Fayard et al. 2004). This is not surprising,

considering the fact that *c*- and *dssurrna* is believed to be transcribed exclusively during mosquito stages (van Spaendonk et al. 2000).

Rescue-transfected parasites had significantly higher growth rates than mock-transfected parasites. It is likely that growth rates of both rescue and mock-transfected parasites were delayed by WR99210 treatment of the mice. De Koning-Ward et al. (2000a) report that the WR99210 resistance of *hdhfr*-transfected parasites is related to the *hdhfr* copy number, and that a single copy of *hdhfr* only slightly increases WR99210 resistance compared to *tgdhfr*, which was used as selectable marker for the knockout. They claim that the IC_{50} of WR99210 for a single copy of *tgDHFR* is 3×10^{-9}, while the IC_{50} of WR99210 for a single copy of *hDHFR* is 5×10^{-9}. Such a minimal increase in resistance against the selective treatment makes an influence of this treatment on parasite multiplication rates likely. For this reason I did not compare absolute parasite growth rates of WT and rescue parasites, but their respective relationship to the *hslV*-deficient parasite line undergoing the same treatment (WT vs. *hslV*-KO and rescue vs. mock), which showed in both cases that the *hslV*-deficient parasites grew significantly slower than parasites expressing *hslV* (see fig. 11).

8.2 PbHslV / ClpQ expression influences survival time of the host

CD1™ and C57BL/6 mice infected with *hslV*-KO parasites survived significantly longer than WT-infected animals, whereas *hslV*-KO-infected BALB/c mice had a shorter survival time than WT-infected BALB/c (see fig. 8). Strikingly, one out of three *hslV*-KO-infected BALB/c mice showed clear neurological symptoms, i.e. ataxia and seizures, prior to death. Usually BALB/c mice do not develop experimental cerebral malaria (ECM). The triggering of this clinical picture in otherwise ECM resistant animals caused by *hslV* deficiency of the infecting parasites indicates that *hslv* deficiency may lead to changes in pathogenesis.

Griffith et al. (2007) showed in C57BL/6 mice that MyD88 deficiency confers protection against a *P. berghei* infection, whereas in *P. berghei*-infected BALB/c mice, MyD88 deficiency leads to shortened survival times of infected animals and to the development of ECM. Their results in conjunction with the own finding of development of ECM in *hslV*-KO-infected BALB/c mice motivated me to investigate a possible interaction of parasite-*hslV* with host-MyD88 or TLRs.

8.3 Interaction of parasite and innate immune response as a possible explanation for the growth retardation of *hslV*-deficient parasites

The altered growth characteristics of *hslV*-deficient parasites could either be explained by a parasite intrinsic factor or implicate an interrelation of *hslV* and the host's innate immune system.

A fact suggesting immune-mediated growth retardation is the increased spleen weight in *hslV*-KO-infected C57BL/6 mice. Generally, *P. berghei*-infected mice develop a marked splenomegaly during the course of infection (Eling et al. 1977). The spleen is of key importance for the host's resistance against malaria. It is the major site for removal of parasitized erythrocytes, for generation of immunity and for adaptive hematopoiesis (Engwerda et al. 2005). Spleen weight in *hslV*-KO-infected C57BL/6 mice was increased, while parasitemia developed more slowly compared to WT-infected mice. This could be related to an enhanced protective immune response or to sequestration of WBCs with unfavorable immune functions in the spleen caused by the *hslV*-KO parasites. An enhanced immune response in *hslV*-KO-infected mice in turn would suggest an immunosuppressive role of *hslV* or possibly of downstream mediator molecules. The fact that a significant spleen weight increase was only observed in *hslV*-KO C57BL/6 mice, but not in BALB/c or CD1^{TM} outbred mice could imply that this spleen weight increase was mediated by Th1 type immune mechanisms, since C57BL/6, in contrast to BALB/c mice, are believed to mount a Th1 dominated immune response (Mills et al. 2000).

8.4 Proposed interaction of *hslV* and MyD88/TLR-signaling

The innate immune system generally senses PAMPs of invading pathogens through PRRs, which therefore represent potential interaction partners of plasmodial PAMPs. In mammals, Toll-like receptors (TLRs) are the major PRR subgroup. As outlined above, the phenotyping results suggested possible interactions between *hslV* or a *hslV*-derived molecule and TLRs/MyD88. Such an interaction could indicate that *hslV* represents a plasmodial PAMP. As outlined in section 3.4.4, knowledge about

plasmodial PAMPs is still insufficient. This led to the investigation of TLR involvement in host parasite interactions by comparing parasitemia development of WT and *hslV*-KO parasite infections in MyD88-KO mice (see fig.13).

In MyD88-deficient mice, which are regarded as a model for TLR non-functionality, growth retardation of *hslV*-KO parasites compared to WT parasites was not evident. This led to the hypothesis that a linkage of *hslV*-mediated signaling of the parasite and Toll-like receptor signaling of the murine host improved growth conditions for the invading parasite. These beneficial growth conditions were not present in *hslV*-deficient parasites or in a MyD88-deficient host, which would explain the lower parasite growth rates under either of those conditions (see fig. 19).

An additional finding was that growth rates of WT (but not of *hslV*-KO) parasites were considerably higher in normal than in MyD88-deficient C57BL/6 mice. This result further supports the hypothesis of an *hslV*-TLR-mediated parasite growth promotion, but is in contrast to the results of Griffith et al. (2007) and Coban et al. (2007b), who report a similar parasitemia development in normal and MyD88-deficient C57BL/6 mice. It is possible that the here observed differences between normal and MyD88-KO mice were caused by differences between the C57BL/6 lines used, since normal C57BL/6 were obtained from Charles-River-Laboratories and MyD88-deficient C57BL/6 from the MPI, Berlin. For this reason differences were not further evaluated. However, the growth rates of WT parasites in MyD88-KO mice depicted in fig. 13 were reproducible, since the eight WT-infected MyD88-KO mice were infected on two different days with comparable results.

In summary, growth rates of WT and *hslV*-KO parasites in MyD88-KO mice suggest a linkage of parasite-*hslV* and host-TLR-signaling. Specific TLRs or TLR-expressing cell types, which could be involved in such an interaction, remain elusive. There are several publications reporting an inhibition of DC maturation, caused by malaria parasites, which are discussed in section 8.7.

8.5 Possible *hslV* interactions I: The chaperone network of the mitochondrial matrix

How an immune interaction between *hslV* and TLR-signaling could be mediated needs further clarification. Our group recently showed that ClpQ is located within the mitochondrion (Tschan et al. 2010). Furthermore results of the MitoTracker-staining

show that mitochondria appear to have a different shape in *hslV*-KO as in WT *P. berghei* parasites. Analogously it was reported for trypanosoma that RNAi knockdown of trypanosomal *hslV* markedly altered mitochondrial DNA replication, leading to a continuous synthesis of small circular mitochondrial DNA and growth of the mitochondrial DNA complex to an enormous size (Li et al. 2008).

Regarding this mitochondrial localization it seems unlikely that ClpQ is exported to the iRBC surface. It rather suggests that host parasite-interactions either are mediated by downstream mediators of *hslV* or that the protease is liberated during schizont egress (see fig. 19).

One possible explanation for an interaction between ClpQ and the host's immune system could be an exported mediator-molecule processed by ClpQ. In this context it is interesting that Ginsburg (website reference) published a chaperone network of the mitochondrial matrix, which facilitates the cleavage of imported proteins within the mitochondrion and their subsequent export as peptides. It is known that several heat-shock proteins are part of this network. Therefore, it is tempting to speculate that *hslV* could be part of this network.

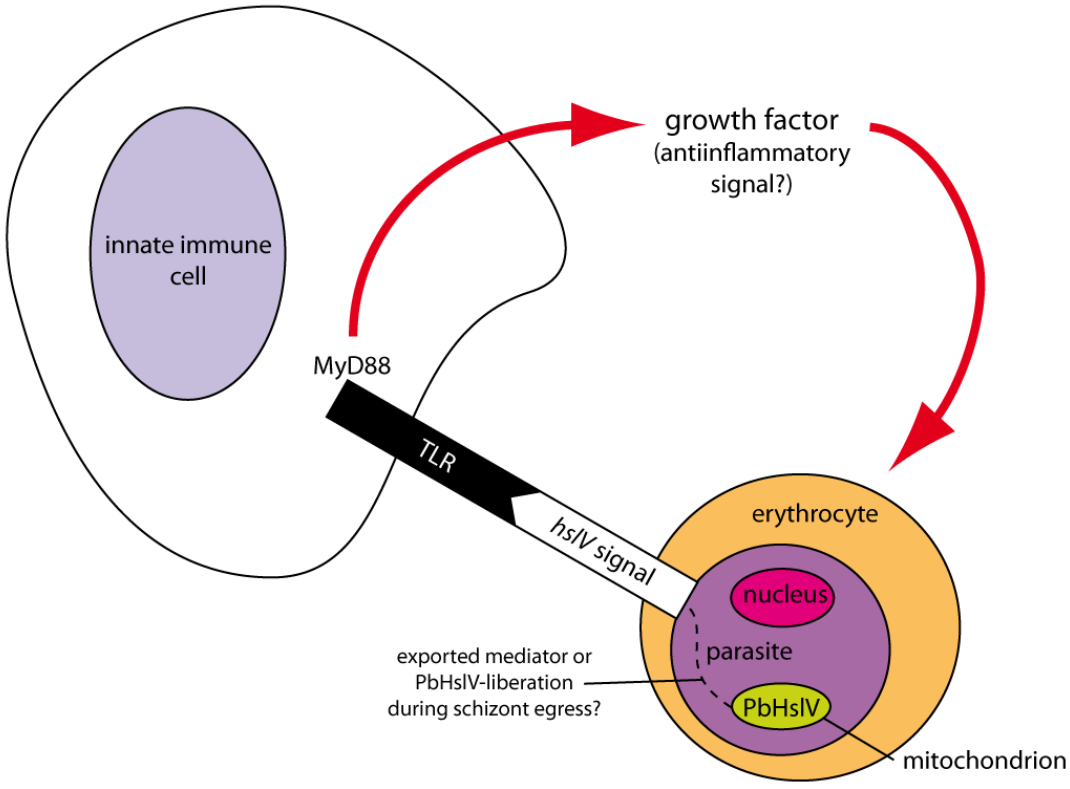

Fig. 19: Proposed interaction of *hslV*-mediated and TLR-mediated signaling.

hslV may be part of a parasite signaling pathway that activates host TLRs, thereby provoking a switch in the host's innate immune response, which supports parasite growth.

8.6 Possible *hslV* interactions II: The innate immune system

Another possible function of *hslV* could be fulfilled during schizont egress. This hypothesis is supported by the exclusive expression of ClpQ during late parasitic stages (late trophozoites and schizonts). An interference with immune functions during this period could facilitate an easier invasion of new RBCs by the released merozoites. An impairment of this mechanism would in turn lead to lower invasion rates thereby explaining the growth retardation of *hslV*-KO parasites.

Ockenhouse et al. (2006) and McCall et al. (2007) used microarrays to investigate PBMC gene-expression profiles during presymptomatic and clinically apparent *P. falciparum* infection. They found an upregulation of several TLRs, MyD88, NF-κB, and IFN-γ in clinically apparent as well as in presymptomatic infections. Similarly, Ropert et al. (2008) describe an initial upregulation of MyD88/TLR-signaling and proinflammatory cytokines in experimental murine malaria. They concluded that MyD88-signaling could be associated with malaria pathogenesis, which fits to the observation of prolonged survival in MyD88-KO mice. Even previous studies with *P. berghei*-infected MyD88-KO mice supported the finding that MyD88-deficiency of the host leads to prolonged survival after infection (Griffith et al. 2007, and Coban et al. 2007b), although these authors did not find any influence of MyD88-deficiency on parasitemia.

Taken together, results from the cited publications suggest that the MyD88/TLR-mediated immune response during early, presymptomatic infection has a detrimental effect on the host. If one assumes an interaction between *hslV* and MyD88/TLR signaling, such an effect could explain the growth retardation of *hslV*-KO parasites as well as that of WT parasites in MyD88-deficient mice.

8.7 Possible interactions between TLRs and iRBCs

The pathways through which iRBCs and TLRs could interact, still remain elusive. Urban et al. (2001) found a parasite-mediated inhibition of DCs, which subsequently fail to fully activate T cells and shift cytokine secretion from a Th1 type to a Th2 type pattern. They report that DC inhibition is mediated by CD36 and caused by intact iRBCs only, whereas a lysate of iRBCs has no effect, which contradicts the hypothesis of *hslV* liberation during schizont egress. Own experiments showed no differences in serum cytokine levels between *hslV*-KO- and WT-infected mice. This does not generally exclude the presence of distinct cytokine expression patterns as described in this publication. Differences could be restricted to certain cell types, such as splenocytes or certain WBCs or could become evident only after investigation of larger animal numbers or other time frames. *hslV*-mediated DC inhibition by parasitized erythrocytes can therefore be regarded as one possible interaction between *hslV* and the immune system.

TLR-iRBC-interactions could be mediated by surface proteins exported to the surface of the iRBC, which in turn could be processed by *hslV*. Chitnis (2001) reports that the AMA-1 protein of plasmodia is proteolytically processed at the time of schizont rupture, facilitating its expression on the merozoite surface. Since it was not possible to knock out the *ama-1* gene, it is assumed that AMA-1 has an essential function during invasion. Further proteins, related to erythrocyte invasion stated in the same publication include RBPs (reticulocyte binding proteins) and EBPs (erythrocyte binding proteins). EBPs have been shown to be linked to the level of virulence of different *P. yoelii* strains [reviewed by Culleton and Kaneko (2009)]. They state that a mutation within the *P. yoelii* Erythrocyte Binding Like (PyEBL) protein leads to an altered trafficking pathway of this protein (i.e. to the dense granules instead of the micronemes), which subsequently leads to highly increased multiplication rates of the asexual blood stages. Whether or not these molecules are related to *hslV*, requires further clarification.

9 SUMMARY

The protease ClpQ, encoded by the plasmodial gene *hslV* (PB000649.02.0), is a threonine peptidase, expressed by plasmodia during the late blood stages. Due to its highly conserved sequence among *Plasmodium spp*., *hslV* appears to play a fundamental role in plasmodial cell metabolism. This thesis investigates its function by generation and phenotypic characterization of transgenic, *hslV*-deficient *Plasmodium berghei* parasites. *hslV*-deficient parasites showed a substantial growth retardation of the blood stages, which was partially reversed when MyD88-deficient mice were used as a host organism.

An explanation for this phenomenon could be a linkage of *hslV*-mediated signaling of the parasite and Toll-like receptor signaling of the murine host, which leads to improved growth conditions for the invading parasite. These beneficial environment is probably not provided in *hslV*-deficient parasites or in a MyD88-deficient-host explaining the lower parasite growth rates under those conditions. How these host-parasite-interactions are mediated, is subject of further investigations.

In summary, the obtained results suggest that the protease ClpQ may be involved in the modulation of the host's innate immune response during an infection with *Plasmodium berghei*, which suggests that ClpQ is a candidate for a plasmodial virulence factor. Its absence in the mammalian host makes ClpQ an attractive target for future interventional approaches. Further research to characterize related molecular pathways is needed to clarify its role during the innate immune response especially in view of future vaccine development strategies.

10 ZUSAMMENFASSUNG

Die Protease ClpQ, die durch das plasmodiale Gen *hslV* (PB000649.02.0) kodiert wird, ist eine Threoninpeptidase, die von späten Blutstadien der Plasmodien exprimiert wird. Aufgrund seiner in *Plasmodium spp.* hochkonservierten Sequenz, scheint *hslV* für den Zellstoffwechsel der Parasiten von grundlegender Bedeutung zu sein. In dieser Arbeit wurde die Funktion von ClpQ anhand eines *hslV*-Knockouts in *Plasmodium berghei* und nachfolgender Phänotypisierung der Knockout-Parasiten untersucht. *hslV*-defiziente Parasiten zeigten erheblich reduzierte Vermehrungsraten der Blutstadien. Dieser Phänotyp war bei der Infektion von MyD88-Knockout-Mäusen mit WT- und *hslV*-KO-Parasiten nicht signifikant nachweisbar.

Das Phänomen ließe sich durch eine Interaktion von plasmodialem *hslV* mit Toll-like Rezeptoren des Wirtsorganismus, die zu verbesserten Wachstumsbedingungen für den Parasiten führt, erklären. Diese verbesserten Wachstumsbedingungen fehlen in *hslV*-defizienten Parasiten oder einem MyD88-defizienten Wirtsorganismus, was die reduzierten Vermehrungsraten unter diesen Bedingungen erklären würde. Welche Signalübertragungswege eine solche Parasit-Wirt-Interaktion vermitteln könnten, ist Gegenstand nachfolgender Studien.

Zusammengenommen weisen die Ergebnisse dieser Arbeit darauf hin, dass ClpQ an der Interaktion des Malariaparasiten mit dem angeborenen Immunsystem des Wirtsorganismus beteiligt ist und dass es sich somit bei *hslV* um einen möglichen plasmodialen Virulenzfaktor handelt.

Die Tatsache, dass ClpQ im Wirtsorganismus nicht vorkommt, macht die Protease zu einem vielversprechenden Zielmolekül für zukünftige Malariatherapeutika bzw. zu einem Impfantigenkandidaten. Im Hinblick auf zukünftige Ansätze zur Malariabehandlung oder –prophylaxe, sollte durch weitere Experimente geklärt werden, welche Signaltransduktionswege in diesem Zusammenhang von Bedeutung sind.

11 ACKNOWLEDGEMENT

I first want to thank my supervisors Dr. Benjamin Mordmüller and Prof. Dr. Christoph Grevelding for their continuous scientific and personal support throughout the work on my thesis. I am still glad to have found you as supervisors.

Furthermore, I thank my second supervisor Prof. Dr. Jürgen Kun for supporting me during the last phase of my dissertation and for skipping one day of christmas cookie eating for a snow trip to Gießen to make my examination possible. I thank my colleagues Andrea, Serena, Jana, Rolf, Ulrike, Meral and Anthony for helpful comments and for being friends during the time of my thesis. Finally, I want to thank I thank Prof. Dr. PG. Kremsner for having me in his institute, Dr. Wolfgang Hoffmann from our institute for assistance with the i.v. injections of the mice, and Dr. Uwe Klemm (Max-Planck-Institut f. Infektionsbiologie, Berlin, Germany) for providing the MyD88 knockout mice.

12 REFERENCES

Akashi-Takamura, S. and Miyake, K., 2008. TLR accessory molecules. *Current Opinion in Immunology*, 20(4), 420-425.

Areschoug, T. and Gordon, S., 2009. Scavenger receptors: role in innate immunity and microbial pathogenesis. *Cellular Microbiology*. 2009 Aug;11(8):1160-9.

Arrighi, R.B.G. and Faye, I., 2009. *Plasmodium falciparum* GPI toxin: A common foe for man and mosquito. *Acta Tropica*. 2010 Jun;114(3):162-5.

Bafort, J., Timperman, G. and Delbar, T., 1968. Observation on tissue schizogony and sporogony of rodent malaria. *Annales des sociétés belges de médecine tropicale, de parasitologie, et de mycologie*, 48(5), 535-540.

Baird, J.K., 2009. Malaria zoonoses. *Travel Medicine and Infectious Disease*, 7(5), 269-277.

Balu, B. and Adams, J.H., 2007. Advancements in transfection technologies for *Plasmodium*. *International Journal for Parasitology*, 37(1), 1-10.

Bochtler, M. et al., 2000. The structures of HsIU and the ATP-dependent protease HsIU-HsIV. *Nature*, 403(6771), 800-805.

Boothroyd, J.C., 2009. Expansion of host range as a driving force in the evolution of Toxoplasma. *Memórias Do Instituto Oswaldo Cruz*, 104(2), 179-184.

Chitnis, C.E., 2001. Molecular insights into receptors used by malaria parasites for erythrocyte invasion. *Current Opinion in Hematology*, 8(2), 85-91.

Coban, C. et al., 2005. Toll-like receptor 9 mediates innate immune activation by the malaria pigment hemozoin. *The Journal of Experimental Medicine*, 201(1), 19-25.

Coban, C. et al., 2007a. Manipulation of host innate immune responses by the

malaria parasite. *Trends in Microbiology*, 15(6), 271-278.

Coban, C. et al., 2007b. Pathological role of Toll-like receptor signaling in cerebral malaria. *International Immunology*, 19(1), 67-79.

Coleman, B.I. and Duraisingh, M.T., 2008. Transcriptional control and gene silencing in *Plasmodium falciparum*. *Cellular Microbiology*, 10(10), 1935-1946.

Culleton, R. and Kaneko, O., 2009. Erythrocyte binding ligands in malaria parasites: Intracellular trafficking and parasite virulence. *Acta Tropica*, 2010 Jun;114(3):131-7.

Deitsch, K. et al., 2007. Mechanisms of gene regulation in *Plasmodium*. *The American Journal of Tropical Medicine and Hygiene*, 77(2), 201-208.

Delves, P.J. and Roitt, I.M., 2000. The immune system. First of two parts. *The New England Journal of Medicine*, 343(1), 37-49.

Eling, W., van Zon, A. and Jerusalem, C., 1977. The course of a *Plasmodium berghei* infection in six different mouse strains. *Zeitschrift Für Parasitenkunde (Berlin, Germany)*, 54(1), 29-45.

Elofsson, M. et al., 1999. Towards subunit-specific proteasome inhibitors: synthesis and evaluation of peptide alpha',beta'-epoxyketones. *Chemistry and Biology*, 6(11), 811-822.

Engwerda, C.R., Beattie, L. and Amante, F.H., 2005. The importance of the spleen in malaria. *Trends in Parasitology*, 21(2), 75-80.

Franke-Fayard, B. et al., 2005. Murine malaria parasite sequestration: CD36 is the major receptor, but cerebral pathology is unlinked to sequestration. *Proceedings of the National Academy of Sciences of the United States of America*, 102(32), 11468-11473.

Franke-Fayard, B. et al., 2004. A *Plasmodium berghei* reference line that constitutively expresses GFP at a high level throughout the complete life cycle. *Molecular and Biochemical Parasitology*, 137(1), 23-33.

Franklin, B.S. et al., 2009. Malaria primes the innate immune response due to interferon-gamma induced enhancement of toll-like receptor expression

and function. *Proceedings of the National Academy of Sciences of the United States of America*, 106(14), 5789-5794.

Freeman, R.R. and Parish, C.R., 1978. Spleen cell changes during fatal and self-limiting malarial infections of mice. *Immunology*, 35(3), 479-484.

Gille, C. et al., 2003. A comprehensive view on proteasomal sequences: implications for the evolution of the proteasome. *Journal of Molecular Biology*, 326(5), 1437-1448.

Ginsburg, H., Malaria Parasite Metabolic Pathways: Chaperone network of the mitochondrial matrix. Available at: http://sites.huji.ac.il/malaria/maps/chaperone.html

Global Malaria Action Plan. Available at: http://www.rollbackmalaria.org/gmap

Gowda, D.C., 2007. TLR-mediated cell signaling by malaria GPIs. *Trends in Parasitology*, 23(12), 596-604.

Griffith, J.W. et al., 2007. Toll-like receptor modulation of murine cerebral malaria is dependent on the genetic background of the host. *The Journal of Infectious Diseases*, 196(10), 1553-64.

Griffith, J.W. et al., 2009. Pure hemozoin is inflammatory *in vivo* and activates the NALP3 inflammasome via release of uric acid. *Journal of Immunology*, 183(8), 5208-5220.

Groll, M. et al., 2005. Molecular machines for protein degradation. *Chembiochem: A European Journal of Chemical Biology*, 6(2), 222-256.

Hanum P, S., Hayano, M. and Kojima, S., 2003. Cytokine and chemokine responses in a cerebral malaria-susceptible or -resistant strain of mice to *Plasmodium berghei* ANKA infection: early chemokine expression in the brain. *International Immunology*, 15(5), 633-640.

Ishii, K.J. et al., 2008. Host innate immune receptors and beyond: making sense of microbial infections. *Cell Host and Microbe*, 3(6), 352-363.

Janse, C.J., Ramesar, J. and Waters, A.P., 2006. High-efficiency transfection and drug selection of genetically transformed blood stages of the

rodent malaria parasite *Plasmodium berghei*. *Nature Protocols*, 1(1), 346-356.

Kilama, W. and Ntoumi, F., 2009. Malaria: a research agenda for the eradication era. *The Lancet*, 374(9700), 1480-1482.

de Koning-Ward, T.F., Fidock, D.A. et al., 2000a. The selectable marker human dihydrofolate reductase enables sequential genetic manipulation of the *Plasmodium berghei* genome. *Molecular and Biochemical Parasitology*, 106(2), 199-212.

de Koning-Ward, T.F., Janse, C.J. and Waters, A.P., 2000b. The development of genetic tools for dissecting the biology of malaria parasites. *Annual Review of Microbiology*, 54, 157-185.

Kreidenweiss, A., Kremsner, P.G. and Mordmüller, B., 2008. Comprehensive study of proteasome inhibitors against *Plasmodium falciparum* laboratory strains and field isolates from Gabon. *Malaria Journal*, 7, 187.

Langhorne, J. et al., 2008. Immunity to malaria: more questions than answers. *Nature Immunology*, 9(7), 725-732.

Li, Z. et al., 2008. Identification of a bacterial-like HslVU protease in the mitochondria of *Trypanosoma brucei* and its role in mitochondrial DNA replication. *PLoS Pathogens*, 4(4), e1000048.

Maggio-Price, L., Brookoff, D. and Weiss, L., 1985. Changes in hematopoietic stem cells in bone marrow of mice with *Plasmodium berghei* malaria. *Blood*, (66(5)), 1080-5.

Martinsen, E.S., Perkins, S.L. and Schall, J.J., 2008. A three-genome phylogeny of malaria parasites (*Plasmodium* and closely related genera): evolution of life-history traits and host switches. *Molecular Phylogenetics and Evolution*, 47(1), 261-273.

McCall, M.B.B. et al., 2007. *Plasmodium falciparum* infection causes proinflammatory priming of human TLR responses. *Journal of Immunology*, 179(1), 162-171.

Medzhitov, R., 2007. Recognition of microorganisms and activation of the

immune response. *Nature*, 449(7164), 819-826.

Mills, C.D. et al., 2000. M-1/M-2 macrophages and the Th1/Th2 paradigm. *Journal of Immunology*, 164(12), 6166-6173.

Mordmüller, B. et al., 2006. Plasmodia express two threonine-peptidase complexes during asexual development. *Molecular and Biochemical Parasitology*, 148(1), 79-85.

Ockenhouse, C.F. et al., 2006. Common and divergent immune response signaling pathways discovered in peripheral blood mononuclear cell gene expression patterns in presymptomatic and clinically apparent malaria. *Infection and Immunity*, 74(10), 5561-5573.

Parroche, P. et al., 2007. Malaria hemozoin is immunologically inert but radically enhances innate responses by presenting malaria DNA to Toll-like receptor 9. *Proceedings of the National Academy of Sciences*, 104(6), 1919-1924.

P. berghei - Plasmids for genetic modification. Available at: http://www.lumc.nl/con/1040/81028091348221/810281121192556/811070931392556

Powers, J.C. et al., 2002. Irreversible inhibitors of serine, cysteine, and threonine proteases. *Chemical Reviews*, 102(12), 4639-4750.

Rasmussen, S.B., Reinert, L.S. and Paludan, S.R., 2009. Innate recognition of intracellular pathogens: detection and activation of the first line of defense. *APMIS: Acta Pathologica, Microbiologica, Et Immunologica Scandinavica*, 117(5-6), 323-337.

Ropert, C., Franklin, B.S. and Gazzinelli, R.T., 2008. Role of TLRs/MyD88 in host resistance and pathogenesis during protozoan infection: lessons from malaria. *Seminars in Immunopathology*, 30(1), 41-51.

Schoenfeld, D., 1981. The asymptotic properties of nonparametric tests for comparing survival distributions. *Biometrika*, 68, 316-319.

Serghides, L. et al., 2003. CD36 and malaria: friends or foes? *Trends in Parasitology*, 19(10), 461-469.

van Spaendonk, R.M. et al., 2000. The rodent malaria parasite *Plasmodium berghei* does not contain a typical O-type small subunit ribosomal RNA gene. *Molecular and Biochemical Parasitology*, 105(1), 169-174.

Stevenson, M.M. and Riley, E.M., 2004. Innate immunity to malaria. *Nature Reviews. Immunology*, 4(3), 169-180.

Stich, A., 2009. The most important tropical infectious disease. Malaria. *Pharmazie in Unserer Zeit*, 38(6), 508-511.

Thathy, V. and Ménard, R., 2002. Gene targeting in *Plasmodium berghei*. *Methods in Molecular Medicine*, 72, 317-331.

Tomas, A.M. et al., 1998. Transfection systems for animal models of malaria. *Parasitology Today*, 14(6), 245-249.

Tschan, S et al., 2010. Mitochondrial localization of the threonine peptidase PfHslV, a ClpQ ortholog in *Plasmodium falciparum*. *Int J Parasitol.* 2010 Jun 16. [Epub ahead of print], PMID: 20561525

Urban, B.C., Willcox, N. and Roberts, D.J., 2001. A role for CD36 in the regulation of dendritic cell function. *Proceedings of the National Academy of Sciences of the United States of America*, 98(15), 8750-8755.

Urban, B.C. and Todryk, S., 2006. Malaria pigment paralyzes dendritic cells. *Journal of Biology*, 5(2), 4.

Waters, A.P. et al., 1997. Transfection of malaria parasites. *Methods (San Diego, Calif.)*, 13(2), 134-147.

Wells, T.N.C., Alonso, P.L. and Gutteridge, W.E., 2009. New medicines to improve control and contribute to the eradication of malaria. *Nature Reviews. Drug Discovery*, 8(11), 879-891.

WHO, World Malaria Report 2009. Available at: http://www.who.int/malaria/world_malaria_report_2009/en/index.html

13 ERKLÄRUNG

Ich habe die vorgelegte Dissertation selbstständig und ohne unerlaubte fremde Hilfe und nur mit den Hilfen angefertigt, die ich in der Dissertation angegeben habe. Alle Textstellen, die wörtlich oder sinngemäß aus veröffentlichten oder nicht veröffentlichten Schriften entnommen sind, und alle Angaben, die auf mündlichen Auskünften beruhen, sind als solche kenntlich gemacht. Bei den von mir durchgeführten und in der Dissertation erwähnten Untersuchungen habe ich die Grundsätze guter wissenschaftlicher Praxis, wie sie in der "Satzung der Justus-Liebig-Universität Gießen zur Sicherung guter wissenschaftlicher Praxis" niedergelegt sind, eingehalten.

Tübingen, den 08.01.2010

Tanja Paquet-Durand